

IDENTIFICATION AND CONTROL OF INDUSTRIAL GAS FIRED HEAT TREATMENT BATCH FURNACES

A Thesis

Presented in Partial Fulfillment of the Requirements for the

Degree of Master of Science

with a

Major in Electrical Engineering

in the

College of Graduate Studies

University of Idaho

by

Arthur D. Peck

Major Professor: Dakota Roberson, Ph.D.

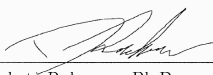
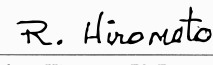
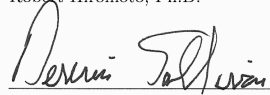
Committee Members: Robert Hiromoto, Ph.D.; Dennis Sullivan, Ph.D., P.E.

Department Administrator: Joe Law, Ph.D., P.E.

December 2020

AUTHORIZATION TO SUBMIT THESIS

This thesis of Arthur D. Peck, submitted for the degree of Master of Science with a Major in Electrical Engineering and titled "Identification and Control of Industrial Heat Treatment Box Furnaces," has been reviewed in final form. Permission, as indicated by the signatures and dates below is now granted to submit final copies for the College of Graduate Studies for approval.

Advisor:	 _____	07 DEC 2020 _____
	Dakota Roberson, Ph.D.	Date
Committee Members:	 _____	10 DEC 2020 _____
	Robert Hiromoto, Ph.D.	Date
	 _____	7 Dec 2020 _____
	Dennis Sullivan, Ph.D., P.E.	Date
Department Chair:	_____	_____
	Joe Law, Ph.D., P.E.	Date

ABSTRACT

This thesis presents methods of system identification and frequency domain control for industrial heat treatment gas powered box furnaces with an emphasis on conforming with Temperature Uniformity Survey (TUS) requirements. While the findings are generically applicable to gas powered heat treatment furnaces information from a specific furnace was used as a source of data and model validation. Two methods of system identification are explored. First is a model derived from thermodynamic principles and furnace geometry, and the second is an output error method using production setpoint/output data. Control systems for each model are designed, and analyzed with respect to temporal performance and global stability.

ACKNOWLEDGEMENTS

I would like to thank Dr. Dakota Roberson for all his hard work and help both with this thesis and my future plans. Without his input and guidance I would not have been able to put together this thesis or have an understanding of how to conduct research. Dr. Roberson's passion for teaching has catalyzed my enjoyment of this program and greatly influenced my future plans.

Hayden Peck gave me the idea for this thesis and provided the furnace data used to generate and validate the models. On top of that he has supported all my needs for additional information, and been a most excellent brother.

TABLE OF CONTENTS

AUTHORIZATION TO SUBMIT THESIS	ii
ABSTRACT	iii
ACKNOWLEDGEMENTS	iv
TABLE OF CONTENTS	v
LIST OF FIGURES	vi
LIST OF ACRONYMS	vii
CHAPTER 1: INTRODUCTION	1
PLANT DESCRIPTION	2
CHAPTER 2: SYSTEM IDENTIFICATION	9
OUTPUT ERROR SYSTEM IDENTIFICATION	9
THERMODYNAMIC PRINCIPLES SYSTEM IDENTIFICATION	12
CHAPTER 3: CONTROLLER DESIGN AND RESULTS	20
PID CONTROLLER	20
MIMO ROBUST CONTROLLER	27
CHAPTER 4: STABILITY ANALYSIS	29
PID CONTROLLER	29
MIMO ROBUST CONTROLLER	34
CHAPTER 5: SUMMARY AND CONCLUSIONS	36
REFERENCES	38

LIST OF FIGURES

1.1	Closed Loop PID Controller Block Diagram	3
1.2	Sensor Block Diagram	4
1.3	Production Temperature Data	5
1.4	Furnace Top View	6
1.5	Furnace Side View	7
1.6	Furnace End View	8
2.1	Closed Loop Model Comparison	10
2.2	TUS Data	15
2.3	Time Domain Model Simulation	16
2.4	Frequency Domain Model Simulation	18
3.1	Starting PID Configuration All TC Response to $1775^{\circ}F$ Step Input	21
3.2	Starting PID Configuration Control Signal Response to $1775^{\circ}F$ Step Input	22
3.3	Tuned PID Configuration All TC Response to $1775^{\circ}F$ Step Input	23
3.4	Tuned PID Configuration Control Signal Response to $1775^{\circ}F$ Step Input	24
3.5	Average Temp. Signal Configuration All TC Response to $1775^{\circ}F$ Step Input	25
3.6	Average Temp. Configuration Control Signal Response to $1775^{\circ}F$ Step Input	26
3.7	MIMO Closed Loop Step Response	28
4.1	Average Temp. Configuration Control Signal Response to $1775^{\circ}F$ Step Input	30
4.2	Average Temp. Configuration Control Signal Response to $1775^{\circ}F$ Step Input	31
4.3	Average Temp. Configuration Control Signal Response to $1775^{\circ}F$ Step Input	32
4.4	TC_1 Starting Configuration Nyquist Plots	33
4.5	TC_3 Loop Transmission Function Bode Plots	34
4.6	Loop Transmission Function (3,3) Gershgorin Plot	35

LIST OF ACRONYMS

TUS	Temperature Uniformity Survey
TC	Thermocouple
PID	Proportional, Integral, Derivative
MIMO	Multi-Input Multi-Output
TF	Transfer Function
ORHP	Open Right Half Plane

CHAPTER 1: INTRODUCTION

This thesis purposes a methodology for improving the control systems of industrial gas powered batch heat treatment furnaces. Specific importance is given to consistently conforming to Temperature Uniformity Survey (TUS) requirements. The method described is intended to be general for all gas powered heat treatment box furnaces and is validated using production and TUS data from a real furnace. The motivation to improve existing box furnace control technology is to reduce the risk and associated cost of failing a TUS, and to increase the throughput and thus profitability of the furnace.

TUS are the primary method of qualifying and maintaining the qualifications of industrial heat treatment furnaces. These surveys consist of measuring the three-dimensional temperature gradient in a furnace to ensure it conforms with the standard [1]. Failure of a TUS results in loss of all the material that went through the furnace since the last successful survey, typically one month. Reducing the risk of TUS failure, and thus loss of material is a highly profitable endeavor.

An inexpensive, effective method of reducing the risk of TUS failure is through improvement of the feedback control system charged with regulating the furnace's internal temperature. A well-designed control system regulates temperature more accurately, providing resilience against unexpected equipment failures and changing furnace conditions. Additionally, a well-tuned control system can maximize usable furnace volume, and minimize temperature rise times. This study investigates two methods of improving the control system. First is the effectiveness of tuning an existing Proportional, Integral, Derivative (PID) controller. This method has the benefit of not requiring any additional hardware resulting in a low input cost. The second method is the synthesis of a high order controller. This method requires a higher fidelity model, and the potential of new hardware such as additional flow control valves. The benefit of this second controller is significantly better performance.

Furnace design plays an influential role in temperature uniformity, and in prioritization of furnace properties. Heat treatment furnaces are manufactured in several different types (e.g. box, rotary, continuous, vacuum, etc.), sizes, and heating methods (e.g. resistance, inductance, natural gas, and coal). In terms of temperature uniformity and desirable furnace properties, each type exhibits different characteristics and the size of the furnace tends to exacerbate temperature uniformity issues.

Batch furnaces (box, rotary, vacuum) go through more heating and cooling cycles than continuous furnaces, and consequently prioritize minimizing heating and cooling times. Batch furnaces can also take advantage of forced convection because it is desirable to have one constant temperature zone where continuous furnaces attempt to minimize temperature coupling across zones [2]. Vacuum furnaces exhibit a similar coupling problem, but through different mechanisms as discussed in [3]. The specific mechanisms and limitation of the furnace types results in a different set of parameters when discussing the improvement of the control system.

The heating method introduces another set of complications and when discussing control, limitations. The limitations typically manifest in the rate of change and variability of heat input. Alternatively, how fast the heat source can change heat generation in response to temperature overshoot, or during heating cycles, and how consistent the behaviour of the heat source is. In coal fired furnaces the physical dimensions of the coal particles impact the time domain profile of heat release [4].

Prototypical mixing of a solid/gas mixture, such as in a coal fired furnace, is not a given, and deviations

in mixture can result in corresponding spacial temperature variations. Natural gas furnace heat input is primarily a function of natural gas mass flow [5]. As a result control of heat input can be reduced to control of the natural gas flow rate. Induction heating can respond even faster than natural gas, and has none of the mixture issues of physical combustion. However, induction heating does demonstrate some coupling phenomena between close induction elements as discussed in [6].

In the first explored method of control production data from an industrial furnace, and the implemented PID controller of that furnace are used to derive a frequency domain model, and hence Transfer Function (TF), of the furnace and its actuators (gas heaters). The model is then used to test changes to the PID controller.

The second method develops a model of the validation furnace using thermodynamic principles for the combustion, manufacturer data of specific components for actuator saturation points and operational limits, and furnace layout for interactions between actuators and measurement zones.

The controllers are graded in terms of conformance with the TUS standard, rise time, loop feedback magnitude, and stability[1].

To document this process and the results this paper is organized as follows. First the physical characteristics of the furnace, and its starting control system are discussed. The source of data and derivation of the mathematical models are established. The models are validated, and the control schemes adjusted to investigate possible performance improvements. Finally the results are analyzed in terms of time domain response, and stability.

1.1 PLANT DESCRIPTION

The box furnace that provided the data for this study is approximately 25 ft long by 10 ft wide and 8 ft tall with a qualified working volume of 18 ft long by 4 ft wide by 2 ft tall. The furnace has 10 natural gas heaters (actuators). During production, temperature is measured using 8 equally spaced Thermocouples (TCs). The TCs are arranged in a single plane with 4 TCs per long side see Figs. 1.4, 1.5, and 1.6. The furnace is a Class 1 furnace which is required to maintain temperature within a $5^\circ F$ band of the steady state temperature [1]. This requirement primarily limits usable furnace volume and minimum heat up times.

The furnace regulates temperature via a closed loop PID controller with a standard feedback configuration found in Fig. 1.1. The controller is implemented by an Allen-Bradley SLC 500 programmable logic controller.

The feedback signal in Fig. 1.1, is taken as the *maximum* temperature of the 8 TCs as shown in Fig. 1.2. The use of a single TC to control all the actuators increases undesirable coupling which invariably produces a temperature gradient due to the disparate geometric positions of the TCs.

Generally, the set of measurements simultaneously collected by N sensors at time t are given as

$$M_t = \{m_1(t), m_2(t), \dots, m_N(t)\}, \forall t \geq 0, M_t \in \mathbb{R}. \quad (1.1)$$

The sensor used to inform actuation, then, is the maximum value of this set, $s(t) = \max[M_t], \forall t \geq 0, s(t) \in \mathbb{R}$.

As an illustrative example, the furnace will have a predisposition toward hot and cold zones due to natural variance in construction and spacial layout of burners; the control system described fails to correct this natural temperature gradient. Additionally, the actuators do not have proportional gas flow; instead they are binary and turned on and off to produce an acceptably constant temperature. These two factors are the primary contributors to the difference between the maximum and minimum temperatures and the steady state oscillation of the furnace Fig. 1.3.

Actuator function is given by

$$A(t) = \begin{cases} 0 & \text{if } s(t) \geq u(t) + \delta \\ 0 & \text{if } u(t) - \delta < s(t) < u(t) + \delta, s'(t) < 1 \\ 1 & \text{if } s(t) \leq u(t) - \delta \\ 1 & \text{if } u(t) - \delta < s(t) < u(t) + \delta, s'(t) > 1 \end{cases}$$

$$\forall t \geq 0, s(t), s'(t), \delta \in \mathbb{R}. \quad (1.2)$$

Where $A(t)$ is the actuator output (on or off), $s(t)$ is the sensor signal as defined above, $s'(t) = \frac{d}{dt}s(t)$ is the first derivative of $s(t)$, $u(t)$ is the setpoint, and δ is the acceptable deviation from the setpoint.

The second control method modifies the plant model by allowing independent and continuous control of each burner, and feeding back all eight TC measurements. This modification allows for elimination of the spacial temperature gradient and of the steady state oscillation. With this modification the sensor measurements remain as shown in (1.1), but the maximum filter is removed. The new actuator model is governed by combustion and is derived in Section 2.2.

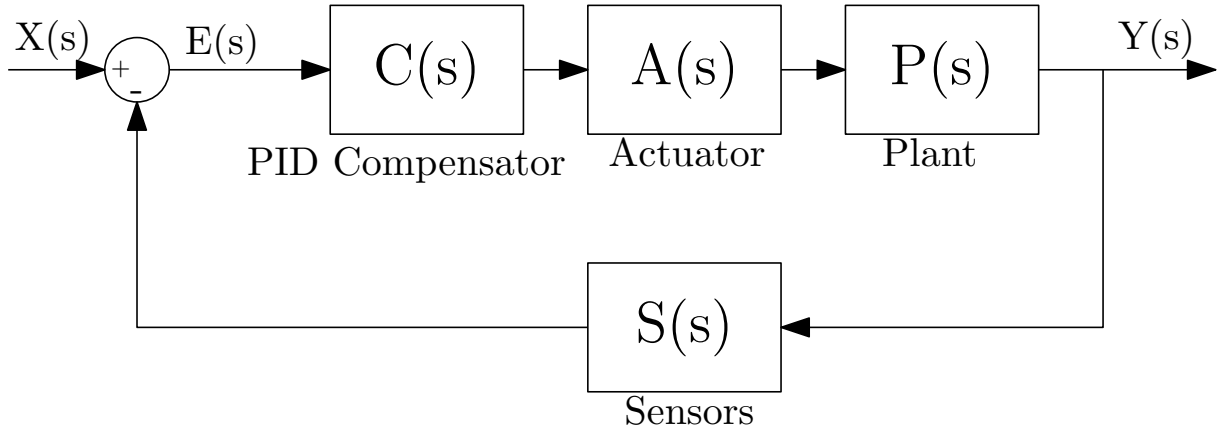


Figure 1.1: Closed Loop PID Controller Block Diagram

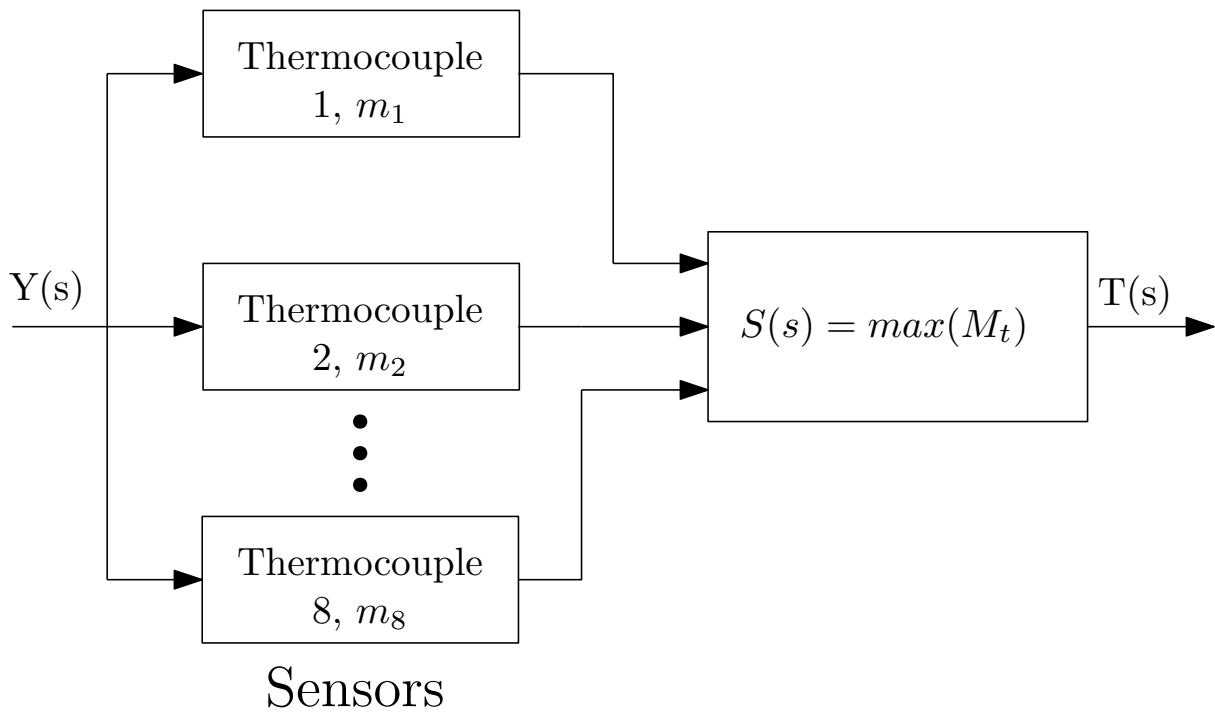


Figure 1.2: Sensor Block Diagram

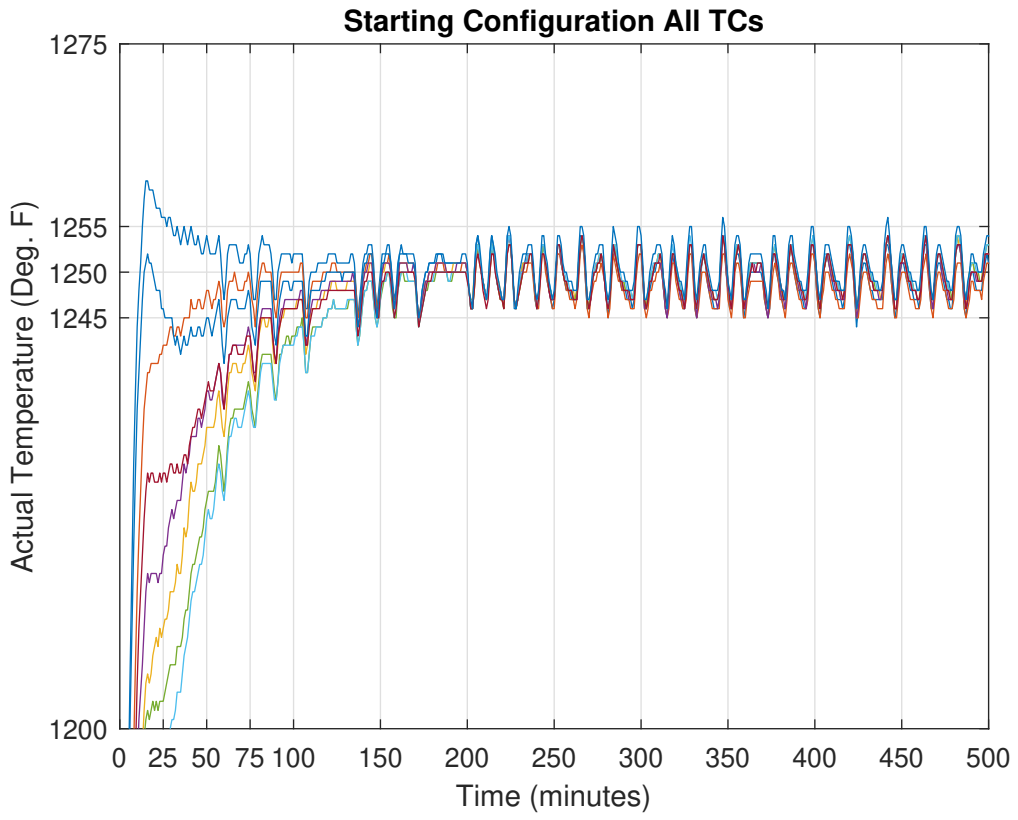
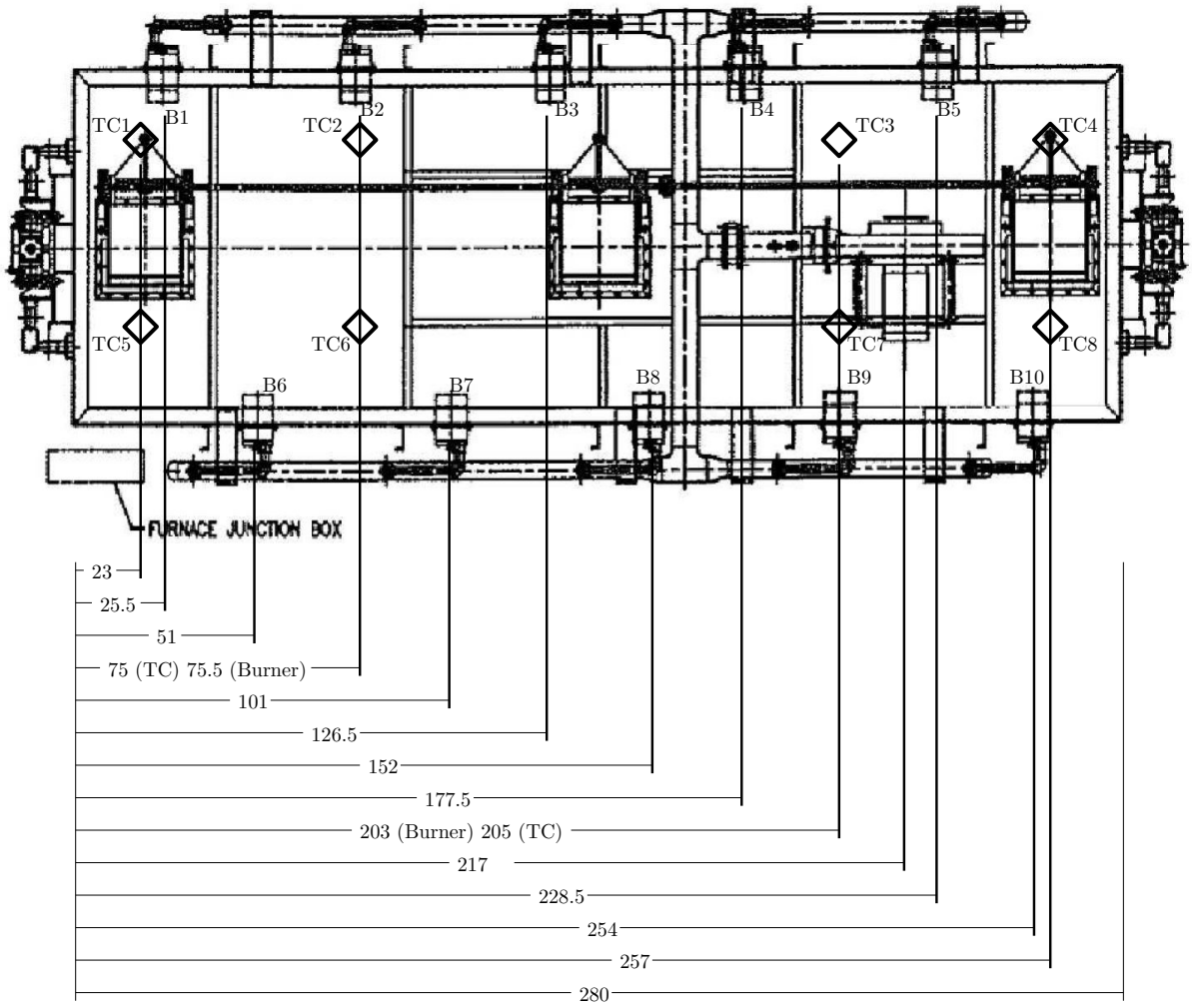


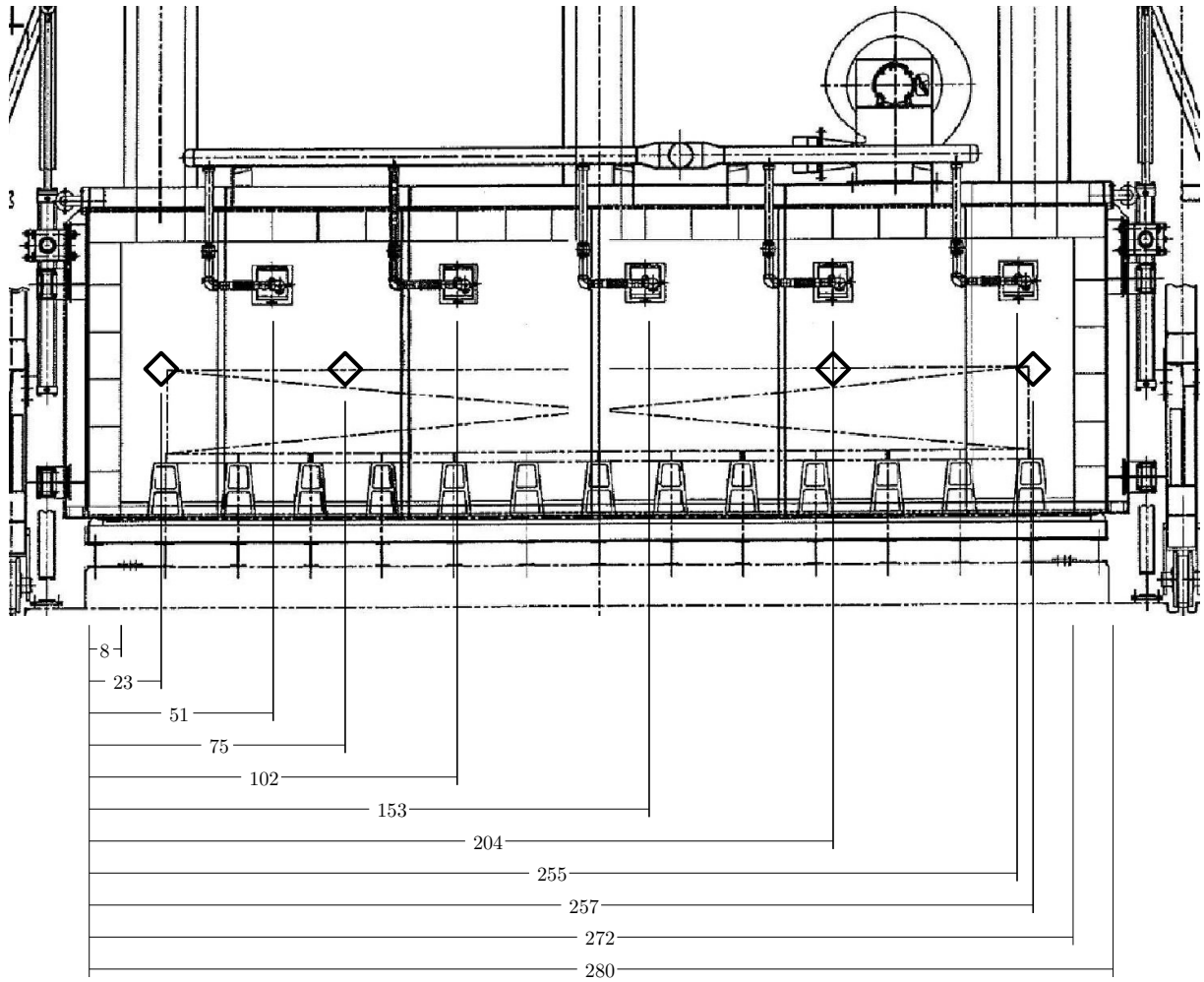
Figure 1.3: Production Temperature Data



All Units in Inches

◇ Represents a Thermocouple

Figure 1.4: Furnace Top View



Units are in inches
◇ Represents a Thermocouple

Figure 1.5: Furnace Side View

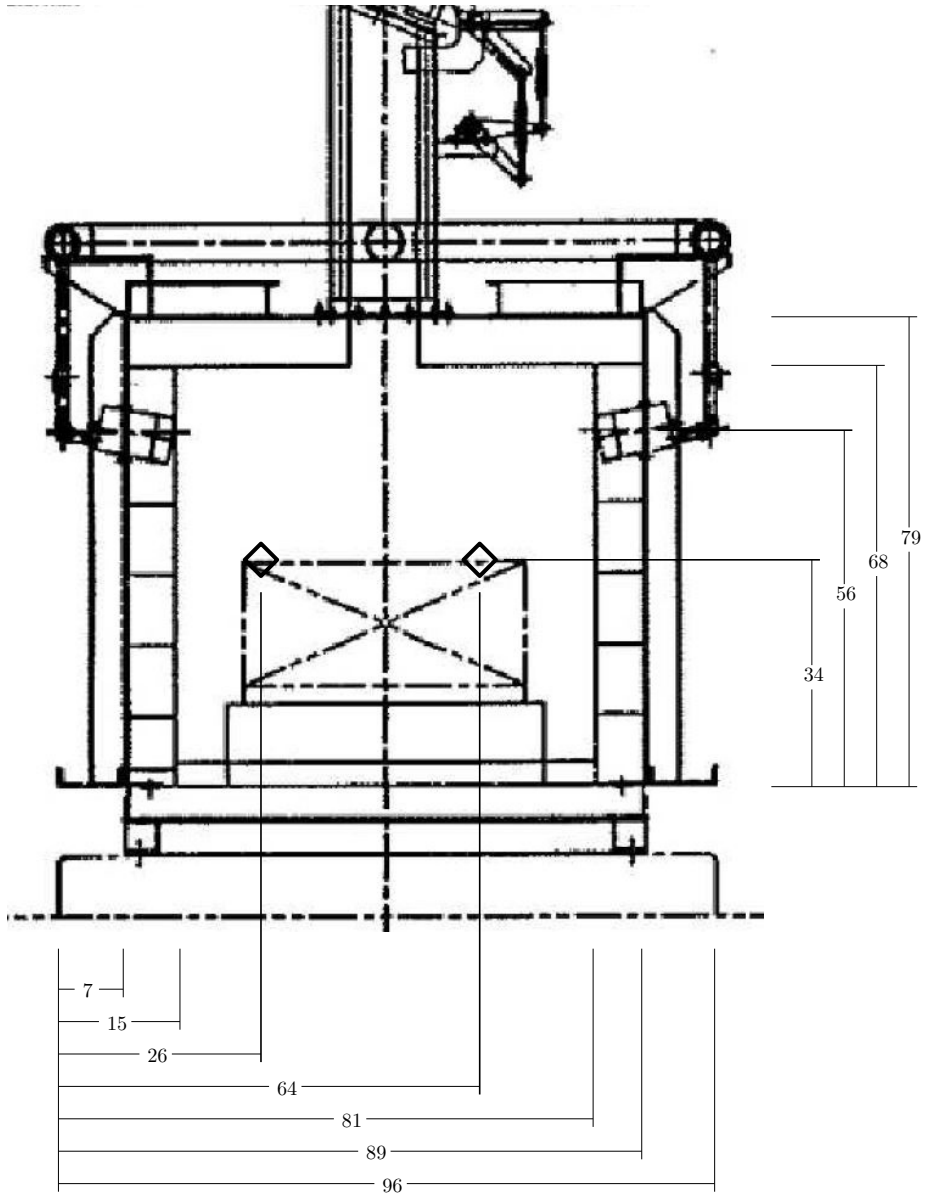


Figure 1.6: Furnace End View

CHAPTER 2: SYSTEM IDENTIFICATION

This chapter presents the two methods of system identification. First is the method used to create a closed loop TF and ultimately tune the existing PID. This is based on a numerical output error method[7]. The second method generates a time domain model using thermodynamic principles, manufacturer information, and furnace layout. This model is tuned using TUS data. The model is then converted to the frequency domain via simulation and a numerical output error method similar to that described above.

2.1 OUTPUT ERROR SYSTEM IDENTIFICATION

The first step in implementing an improved control system is to create a viable mathematical model of the plant and actuators. In this method the model creation process starts with data smoothing, then an output error (OE) method of system identification is used on the processed data producing a closed loop frequency domain TF [7]. *A priori* knowledge of the PID is used to create a separate PID TF that is then factored out of the closed loop TF leaving only the plant/actuator TF. Each of these steps, and known sources of error are discussed in greater detail below.

The data available for this study consists of an entire month of production data; about 55,000 data per TC. Since each TC resides in a spatially unique location each is treated as a separate plant/actuator. Thus the same system identification process is performed eight times, once for each TC. Testing using all 55,000 data simultaneously results in a homogenized TF that misses several key aspects of the furnace. To solve this problem the data is broken into 10 equal segments per TC. The segments are individually passed through an equiripple filter with a sampling frequency of $0.0166Hz$, a passband of $10^{-5}Hz$, and a stopband of $10^{-4}Hz$. These values are chosen in an attempt to filter out the sinusoidal noise with a period of about eight minutes ($0.0021Hz$) as shown in Fig. 1.3. The filtered data is then downcounted by a factor of 10.

An output error method of system identification is then implemented on each set of downcounted data [7]. It was assumed that the transfer functions were 3^{rd} order. This assumption allowed for sufficient flexibility, primarily in response times, but minimized the overfitting concern. A 3^{rd} order TF also accounts for known heat transfer methods while allowing room to capture specific aspects of the furnace. This results in 10 TFs for each TC. Each TC worth of TFs is then combined such that the final TF consists of the most frequently observed poles and zeros. Similar poles and zeros are averaged to create a single pole or zero. This model is checked against the actual production data for accuracy. Fig. 2.1 compares the production data from TC8 to the closed loop TF shown in (2.1). Clearly this model captures the general operation of the plant while ignoring the $0.0021Hz$ sinusoid; this has come at the cost of losing fidelity of the faster, "real" operation.

$$TC_8 = \frac{0.0002955s^3 + 0.000985s^2 + 0.000788s + 0.001871}{s^4 + 0.2509s^3 + 9.869s^2 + 2.472s + 0.001871} \quad (2.1)$$

A generic closed loop model (2.2) is used to factor the plant model, that is the block labeled plant in Fig. 1.1, out of the closed loop model. This method requires *a priori* knowledge of the PID constants, and of the control architecture. The PID constants are $K_p = 6$, $K_i = 66.66$, and $K_d = 33$ which result

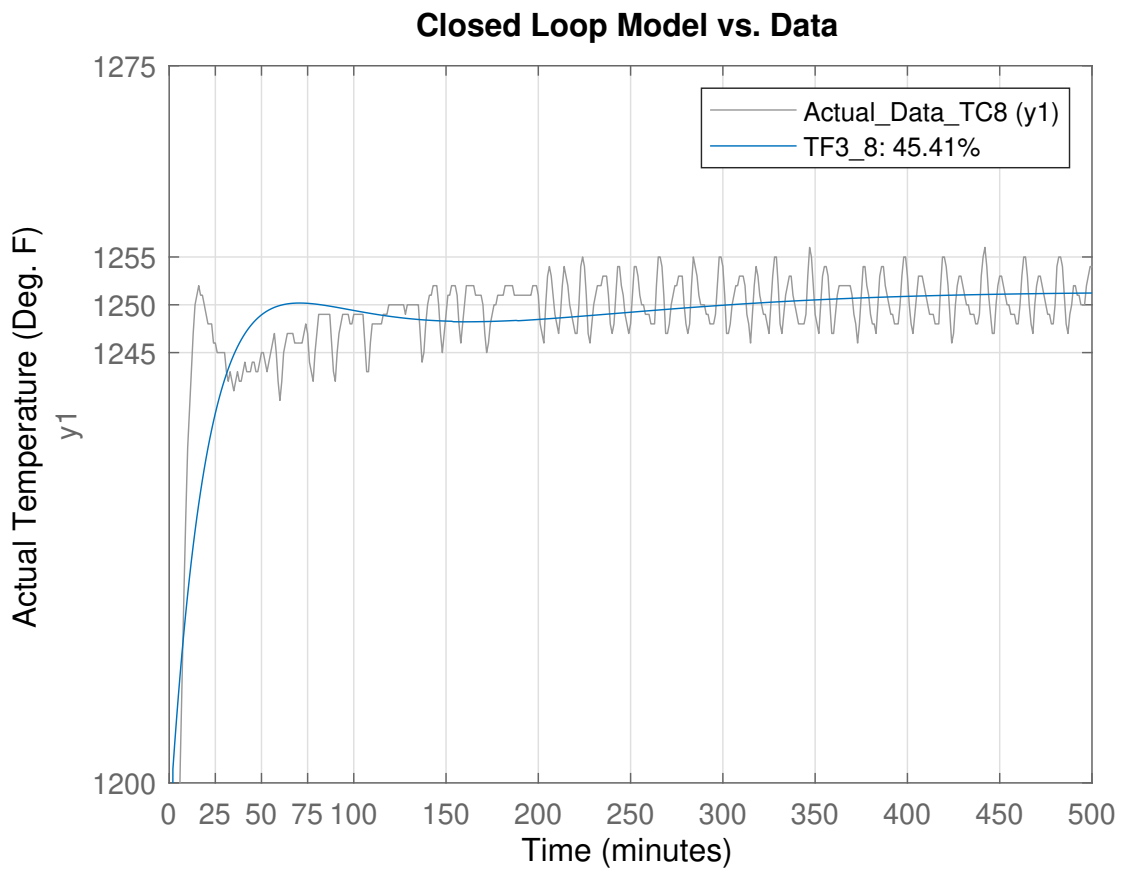


Figure 2.1: Closed Loop Model Comparison

in a TF given by (2.3). To model the use of the maximum temperature value as the control signal, the PID is applied to each plant, TC, independently then the maximum output of these values is used. This model results in each plant being accurately modeled by (2.2) where only the plant values are unique. The plant numerator and denominator are solved as shown in (2.5); the results are shown in (2.13). Note, for this method of modeling the plant models will be referred to by TC_n .

$$CLTF = \frac{PID_n Plant_n}{PID_d Plant_d + PID_n Plant_n} \quad (2.2)$$

where subscript "n" refers to the numerator of the associated TF and subscript "d" refers to the denominator.

$$PID = \frac{33s^2 + 6s + 66.66}{s} \quad (2.3)$$

$$Plant_n = \frac{CLTF_n}{PID_n} \quad (2.4)$$

$$Plant_d = \frac{CLTF_d - PID_n Plant_n}{PID_d} \quad (2.5)$$

$$TC_1 = \frac{0.0002847s + 0.0007061}{s^4 + 0.5006s^3 + 9.921s^2 + 4.939s + 0.5188} \quad (2.6)$$

$$TC_2 = \frac{0.0004347s + 0.0008477}{s^4 + 0.5053s^3 + 9.932s^2 + 4.984s + 0.6242} \quad (2.7)$$

$$TC_3 = \frac{0.001034s + 0.00332}{s^3 + 0.2495s^2 + 9.819s + 2.44} \quad (2.8)$$

$$TC_4 = \frac{0.00244s + 0.006709}{s^3 + 0.5001s^2 + 9.868s + 4.934} \quad (2.9)$$

$$TC_5 = \frac{0.002606s + 0.005343}{s^3 + 0.4075s^2 + 9.872s + 3.933} \quad (2.10)$$

$$TC_6 = \frac{0.0001157s + 0.0003765}{s^4 + 0.3376s^3 + 9.896s^2 + 3.331s + 0.2775} \quad (2.11)$$

$$TC_7 = \frac{0.0004658s + 0.001328}{s^4 + 0.6386s^3 + 9.869s^2 + 6.233s + 0.9779} \quad (2.12)$$

$$TC_8 = \frac{0.00113s + 0.003366}{s^3 + 0.2506s^2 + 9.868s + 2.472} \quad (2.13)$$

The system identification methods did introduce some error into the model. The most obvious error is the inaccuracy of the steady-state oscillation frequency. When comparing Fig. 1.3 and Fig. 3.2 it is clear that the model oscillation is about $0.00833Hz$ while the actual system oscillates at about $0.00166Hz$. This error primarily impacts the accuracy of the rise times; since the magnitude of the oscillations is approximately equal, the difference has no significant effect on steady-state. Control schemes with more flexibility than a PID will experience greater degradation from this error as they are likely attempting a gain stabilization of the pole pair that creates the oscillation. In a similar vein the cooling times (temperature decrease) occur much faster than possible in real life. This is an artifact of the data

available. The "off" signal is a step input to $2^{\circ}F$. The OE method simply uses the input output data, and cannot account for the fact that the furnace has forced heating (gas blowers), but free cooling. Since this study is focused on heating times, and steady-state function the cooling rate error has no significant impact on the findings.

2.2 THERMODYNAMIC PRINCIPLES SYSTEM IDENTIFICATION

In this method the first step is to separate the plant from the actuators and develop a model of each separately. A time domain model of the actuator is developed from the combustion process, and time domain models of the TC zones are developed using the principles of conservation of energy and conservation of mass. The furnace layout is used to determine interaction between TC zones. These time domain models are then joined together again using the furnace layout. The actuator plus plant model is validated by comparison with TUS data. The time domain simulation is then used to generate open loop input/output data for both the actuator and plant. An output error method similar to that described in 2.1 is used to generate frequency domain transfer functions. Each of these processes and sources of error are discussed in the subsequent sections.

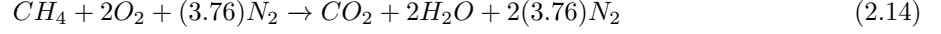
The following assumptions were used to generate this model:

1. Each actuator (burner) is identical.
2. Each actuator can be independently controlled.
3. Gas and air control valves are perfectly controllable.
4. Mass flow into the furnace equals mass flow out of the furnace.
5. The furnace is not loaded with parts.
6. The combustion process is adiabatic.
7. Insulated furnace walls are adiabatic.

The reactants for the actuators used are natural gas and atmospheric air. In the combustion reaction and all necessary physical parameters the natural gas was modeled as methane (CH_4), and air is assumed to be a mixture of oxygen and nitrogen in a 1 : 3.76 ratio. The actuator has three outputs that influence furnace temperature, energy in the form of heat, flame temperature, and mass of the combustion products. It also has three inputs, mass of natural gas, mass of air, and percent theoretical air. Clearly the inputs are interdependent such that controlling any two also controls the third. When considering the relationships with the plant model outputs of flame temperature and total mass are most useful. In generating these outputs the mass of natural gas and air create the simplest relationships. The time domain equations relating mass of reactants to percent theoretical air, flame temperature, and total mass are generated below.

The combustion equation for a stoichiometric mixture of methane with air is given by (2.14)[9]. The stoichiometric mixture is the minimum amount of air needed to consume one mole of methane; this is known as 100% theoretical air. The stoichiometric ratio of moles of methane to moles of air is

approximately 1 : 9.52. The ratio of 1 : 9.74 is given by [10] and was used in this study; (2.17) shows the calculation of percent theoretical air in molar and mass bases. In (2.17) n refers to number of moles and M refers to the molecular weight in $Kg/Kmol$.



$$\%Air_{mol} = \frac{n_{air}}{9.74n_{gas}} \quad (2.15)$$

$$\%Air_{mass} = \frac{n_{air} M_{air}}{9.74n_{gas} M_{gas}} \quad (2.16)$$

$$\%Air_{mass} = \frac{m_{air}}{17.5882m_{gas}} \quad (2.17)$$

The flame temperature is estimated by calculating the adiabatic flame temperature for the subject mixture and applying an scaling constant to account for the process being non-adiabatic. Ideally the scaling constant can be empirically determined; in this case the process is assumed to adiabatic and the adiabatic flame temperature is used. Adiabatic flame temperature is calculated by finding the temperature at which conservation of energy for the reaction is satisfied (2.20) where n refers to the number of moles, \bar{h}_f^o is the enthalpy of formation at $0^\circ C$ and 0.1MPa, $\Delta\bar{h}_i$ is the enthalpy of formation at the actual temperature and pressure, and i refers to reactants while j refers to products. If reactants are at the reference temperature and pressure $\Delta\bar{h}_i$ is zero. The result of (2.20) is that, for a given fuel, the amount of air or percent theoretical air determines the adiabatic flame temperature[9]. Since the enthalpies of formation are experimentally determined they are typically tabulated values. To ease the formulation of a time domain model the adiabatic flame temperature is calculated for percent theoretical air ranged from 100% to 4000% and an exponential of form (2.21) is fit. This range was chosen because it is the range of acceptable conditions of the burner [10].

$$H_R = H_P \quad (2.18)$$

$$H_R = \sum_R n_i (\bar{h}_f^o + \Delta\bar{h})_i \quad (2.19)$$

$$H_P = \sum_R n_j (\bar{h}_f^o + \Delta\bar{h})_j \quad (2.20)$$

$$T_{adi} = Ae^{B*\%Air} + Ce^{D*\%Air} \quad (2.21)$$

The relationship between total mass and the masses of methane and air is straightforward. It satisfies conservation of mass as shown in (2.22). Equations (2.17), (2.21), and (2.22) constitute the time domain model of the actuator with m_{gas} and m_{air} as inputs and m_t and flame temperature as the outputs.

$$m_t = m_{gas} + m_{air} \quad (2.22)$$

To model each TC zone a simple one actuator, one TC volume was considered. The resulting equation was then expanded to consider the contribution to a TC zone from each burner and to account for the interaction between TC zones. The inputs for this model are the flame temperature and total mass of each burner and the outputs are the temperatures of each TC zone resulting in a 20 input, 8 output model.

When considering a single actuator, single TC volume the temperature can be modeled in discrete time through the use of Dalton's model for the mixture of ideal gasses as shown in (2.23)[9]. In (2.23) T_{TC} , T_{adi} , n_{gas} , and n_{air} are the temperature in the TC zone, adiabatic flame temperature, moles of gas, and moles of air at step k while n_{TC} is the moles of gasses in the TC volume. n_{TC} is treated as a constant because all gasses in the TC zone are assumed to be air at all times. This assumption simplifies the evaluation of properties. During simulation this assumption was removed to validate its acceptability. For the furnace used the molecular mass of the gas mixture was equal to the molecular mass of air to two decimal places. When considering furnaces with smaller volumes or different fuel this assumption should be revisited. This model results in an exponential rise to the adiabatic flame temperature. The rate is primarily controlled by the amount of reactants. Equation (2.24) is an equivalent model for continuous time and on a mass rather than molar basis where T_0 is the starting temperature and k_m is a constant used to better fit the equation to known furnace data. Note that k_m modifies the assumption that mass is equal mass out by allowing for some mass to accumulate in the furnace.

$$T_{TC}[k+1] = \frac{(n_{gas}[k] + n_{air}[k])T_{adi}[k] + n_{TC}T_{TC}[k]}{n_{gas}[k] + n_{air}[k] + n_{TC}} \quad (2.23)$$

$$T_{TC}(t) = T_{adi}(t) + (T_0 - T_{adi}(t))e^{\frac{-k_m m_t}{m_{TC}} t} \quad (2.24)$$

Interaction between burners and TC zones is established by inspection of the furnace layout, Fig. 1.4 is useful for this task. This interaction is mathematically shown through the use of constants C_{ij} representing the contribution from the i th burner to the j th TC zone. These constants are bounded such that $\sum_j C_{ij} = 1$ to satisfy the conservation of mass. In (2.24) these constants can be applied directly to the m_t term, but must be normalized for the T_{adi} term resulting in (2.25).

$$T_{TCj}(t) = \frac{\sum_i (C_{ij} T_{adi,i}(t))}{\sum_i C_{ij}} + (T_0 - \frac{\sum_i (C_{ij} T_{adi,i}(t))}{\sum_i C_{ij}}) e^{\frac{-k_m \sum_i (C_{ij} m_{t,i})}{m_{TC}} t} \quad (2.25)$$

Interaction between TC zones is again determined by inspection of the layout. In this case adjacent TC zones interact, and the level of interaction is determined by the shared surface area. This interaction is modeled by applying constants D_{qj} that represent the contribution from the q th TC zone to the j th TC zone. The constants are bounded such that $\sum_q D_{qj} = 1$. The resulting, final equation for time domain temperature of a TC zone is given by (2.26).

$$T_{TCj}(t) = \sum_q [D_{qj} (\frac{\sum_i (C_{ij} T_{adi,i}(t))}{\sum_i C_{ij}} + (T_0 - \frac{\sum_i (C_{ij} T_{adi,i}(t))}{\sum_i C_{ij}}) e^{\frac{-k_m \sum_i (C_{ij} m_{t,i})}{m_{TC}} t})] \quad (2.26)$$

Because the model does not consider a furnace loaded with parts it must be compared to actual TUS data because the TUS is taken in an unloaded furnace. The validation process is further complicated by

the TUS data being in a closed loop. To overcome these difficulties the model is validated by rise time of the hottest TUS TC between approximately $600^{\circ}F$ and $1200^{\circ}F$ which corresponds to about $588^{\circ}K$ and $922^{\circ}K$ respectively. The gas and air flow rates at the time of the TUS are known and the TUS data is shown in Fig. 2.2. These inputs are then used for the model and the results are shown in Fig. 2.3. The rise time of the furnace from the TUS data is between 6 and 8 minutes (TUS samples once every 2 minutes). The rise time of the model is about 9 minutes.

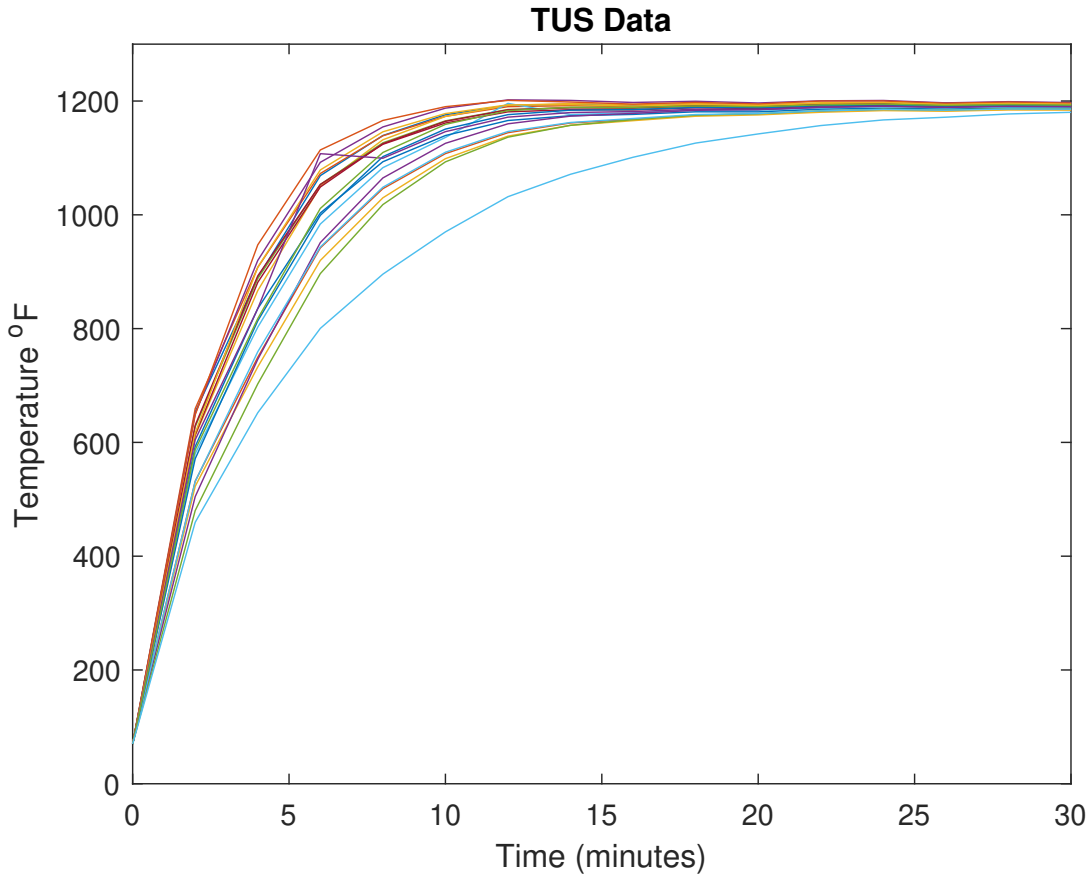


Figure 2.2: TUS Data

Similar to the time domain model the frequency domain model of the burner was developed separate from the plant model. The two were then combined. The frequency domain models are generated by simulation with the time domain model and implementation of an output error method on the simulated input/output data. Ideally each input is excited separately from the rest to accurately model the outputs' dependencies. This is not possible when considering either the burners or the plant because both inputs, m_{gas} and m_{air} , are necessary to produce temperature change. The final result of the frequency domain models are yxu TF matrices where y are the outputs and u are the inputs.

When modeling the burners only the adiabatic flame temperature requires evaluation because the total mass transfer functions are straightforward. To excite the burner m_{gas} and m_{air} are sinusoids

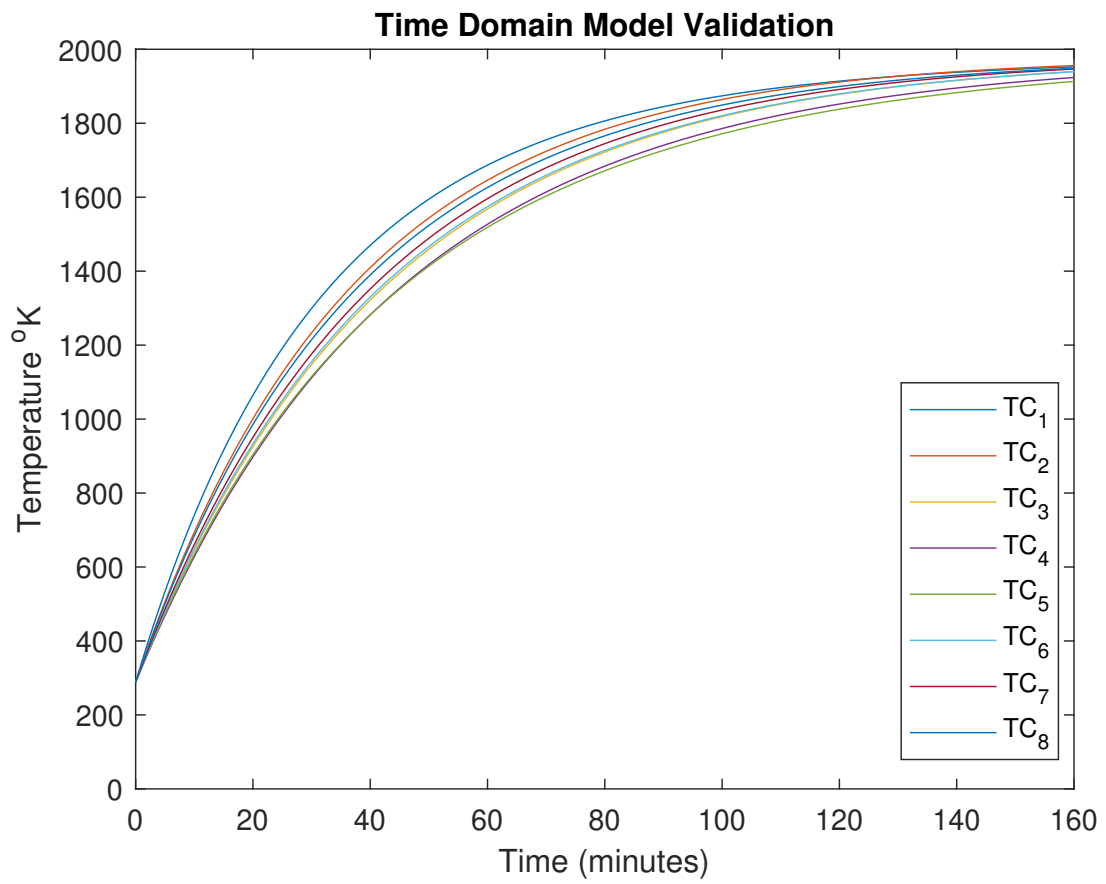


Figure 2.3: Time Domain Model Simulation

oscillating at frequencies that are not integer multiples of each other. The amplitudes are chosen such that they fall within the saturation bounds, but provide a wide range of gas and air combinations. The resulting TF matrix for each burner is shown in (2.27).

$$B_i(s) = \frac{Y(s)}{U(s)} = \begin{bmatrix} \frac{3.19 \cdot 10^6 (s+0.006874)}{s+0.0121} & \frac{-20759(s-0.02722)}{s+0.01221} \\ 1 & 1 \end{bmatrix} \quad (2.27)$$

$$Y(s) = \begin{bmatrix} T_{adi} \\ m_t \end{bmatrix} \quad (2.28)$$

$$U(s) = \begin{bmatrix} m_{gas} \\ m_{air} \end{bmatrix} \quad (2.29)$$

The resulting TF matrix for the entire burner array is:

$$\begin{bmatrix} B_1(s) & 0 & \cdots & \cdots & 0 \\ 0 & B_2(s) & 0 & \cdots & 0 \\ \vdots & & \ddots & & \vdots \\ \vdots & & & \ddots & \vdots \\ 0 & \cdots & \cdots & \cdots & B_{10}(s) \end{bmatrix} \quad (2.30)$$

The plant transfer functions were generated in a similar way. Each burner was excited by the same sinusoidally varying mass flow rates and the plant response to each burner output was determined using the output error method. The transfer function matrix, inputs, and outputs for the entire furnace are given by (2.32) (2.33), and (2.33). Each entry, $TC_{i,j}$, is modeled by a gain and single pole such as in (2.34). The matrices are ordered such that the diagonals of $P(s)$ have the highest gain indicating burner 1 has the greatest influence of TC_1 etc.

$$P(s) = \frac{T_j(s)}{B_i(s)} = \begin{bmatrix} TC_{1,1} & TC_{2,1} & \cdots & TC_{20,1} \\ TC_{1,2} & TC_{2,2} & \cdots & TC_{20,2} \\ \vdots & \vdots & \ddots & \vdots \\ TC_{1,8} & TC_{2,8} & \cdots & TC_{20,8} \end{bmatrix} \quad (2.31)$$

$$B_i(s) = \begin{bmatrix} T_{adi,1} & m_{t,1} & \cdots & T_{adi,10} & m_{t,10} \end{bmatrix}' \quad (2.32)$$

$$T_j(s) = \begin{bmatrix} TC_1 & TC_2 & \cdots & TC_8 \end{bmatrix}' \quad (2.33)$$

$$TC_{1,1} = \frac{0.0011999}{s + .003104} \quad (2.34)$$

The method used to validate the time domain model was used again for the frequency domain model. The system response is shown in Fig. 2.4. The rise time between $588^\circ K$ and $922^\circ K$ is approximately 8 minutes. Therefore the frequency domain model captures the relevant portions of the furnace.

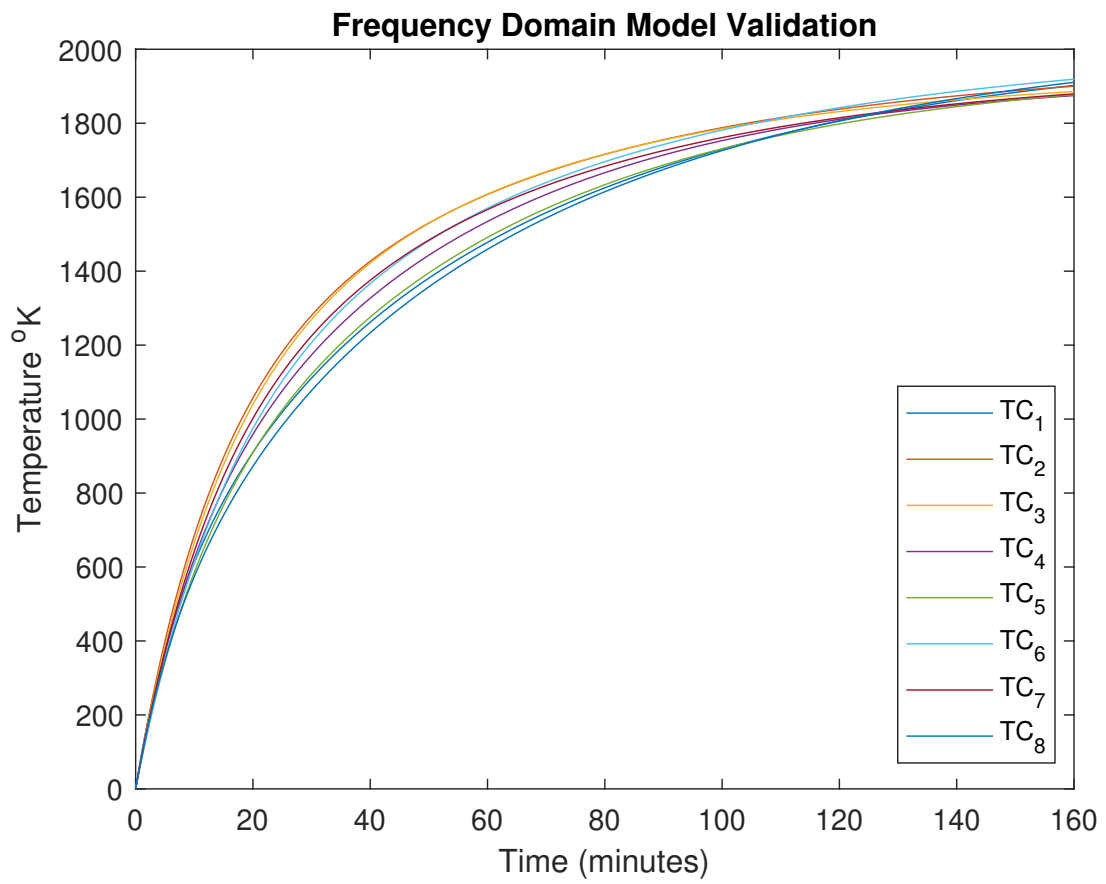


Figure 2.4: Frequency Domain Model Simulation

While the model generated from thermodynamic principles provides many advantages in understanding furnace as a physical system the method of generation does introduce error. One source of error is the overall lack of validation data. The small number of data points from the TUS and the closed loop nature result in losing information about the actual flame temperature given the inputs, and reduces the accuracy of the rise time. The largest risk of error comes from the validity of the assumptions. Assumption 1 is not a large source because all the burners are the same model and were procured/built at the same time minimizing the risk of significant performance differences. To comply with the second and third assumptions the burner needs only be fitted with high quality variable flow valves. The fourth assumption does introduce error because it is likely that combustion products do accumulate in the furnace volume such that mass flow out is less than mass flow in. This error is mitigated by the additions of k_m in (2.24). The assumption that the furnace is not loaded with parts provides a condition for the models such that they will not accurately predict the temperature of a furnace that is loaded with parts. Assumption six does introduce error. It is common in industry to achieve flame temperatures that are several hundred degrees Celsius below the adiabatic flame temperature. Thus by assuming the adiabatic flame temperature is achievable the rise times and maximum possible temperature are affected. Assumption seven is validated by comparing the expected heat loss through the insulated walls to the expected heat loss by air exchange with the outside environment. Heat loss through the walls is determined with the use of manufacturer data and is approximately two orders of magnitude less than heat loss due to mass movement[12]. During any active heating, $T_{adi} > T_{steady-state}$, this heat loss is negligible. During steady-state it will manifest as a very slow decline in temperature that is controllable in the closed loop.

CHAPTER 3: CONTROLLER DESIGN AND RESULTS

The design and performance of both the PID and thermodynamic (Multi-Input Multi-Output (MIMO)) controller are discussed below. The PID is designed to minimize the amount of system change necessary to implement and the MIMO controller is designed to best temporal response. Both controllers are graded on rise time and steady-state error in the time domain, bandwidth in the frequency domain, and stability. Bandwidth and stability of each controller is analyzed in the next chapter. It should be noted that comparison between the PID controllers and the MIMO controller is not valuable because the data used to generate the plant model that is controlled by the PID is from a loaded furnace while the MIMO controller assumes an empty furnace.

3.1 PID CONTROLLER

With a TF for each TC separated from the rest of the system, changes can be made to other portions of the system without further loss of fidelity of the TC behavior. This design uses two different variations in an attempt to reduce temperature rise times, and reduce steady-state error/fluctuation while maintaining adequate stability margin. The first method simply re-tunes the PID to minimize rise time while maintaining a maximum overshoot of $5^\circ F$. The second method changes the feedback logic from using the maximum temperature to using the average temperature of all TCs, and re-tuning the PID to minimize rise time while maintaining a maximum overshoot of $5^\circ F$. All changes are tested using a step input from $2^\circ F$ to $1775^\circ F$, and compared to the identified model's response to the same input, Fig. 3.1 and Fig. 3.2.

Tuning the PID with the given constraints results in a PID TF given by (3.1) where the PID constants are $K_p = 60$, $K_i = 80$, and $K_d = 50$. The resulting step response is given by Fig. 3.3 and Fig. 3.4. This configuration results in about a 20 minute reduction in rise time, but has increased overshoot, and a more sustained steady state oscillation (i.e. slower ringdown). This configuration is in compliance with the uniformity requirements, and at about 20 minutes of savings per heating cycle provides real savings over the initial configuration.

$$PID = \frac{50s^2 + 60s + 80}{s} \quad (3.1)$$

Replacing the maximum feedback signal with an average feedback signal, and re-tuning the PID results in PID constants of $K_p = 8$, $K_i = 40$, and $K_d = 30$, and a TF shown by (3.2). The step response of this control architecture is given by Fig. 3.5 and Fig. 3.6. This setup results in a rise time about 8 minutes slower than the starting configuration, and an overshoot on the highest temperature that exceeded the target ($5^\circ F$). However, this setup "pushes" the TFs toward the target value resulting in a smaller temperature gradient. While this configuration is likely poor for most production environments, the discovery that it reduces the temperature gradient could be important in the development of any hybrid control scheme.

$$PID = \frac{30s^2 + 8s + 40}{s} \quad (3.2)$$

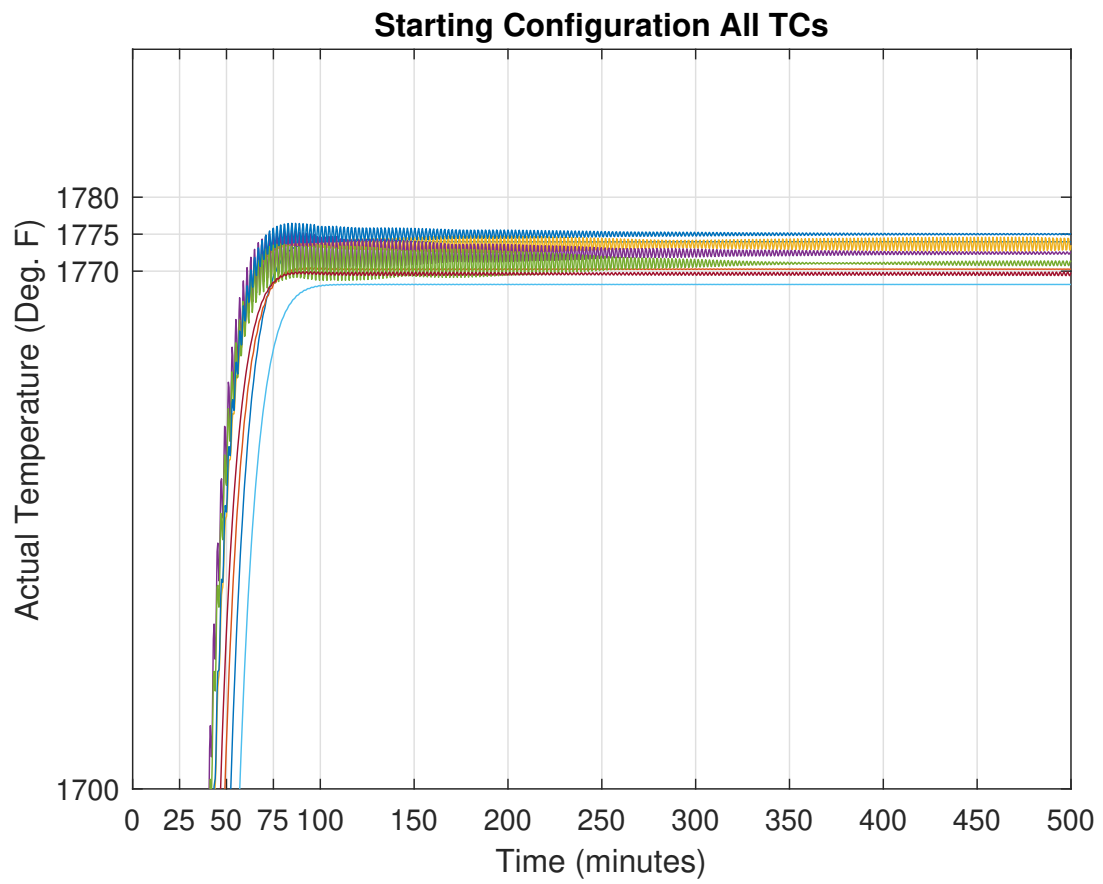


Figure 3.1: Starting PID Configuration All TC Response to 1775°F Step Input

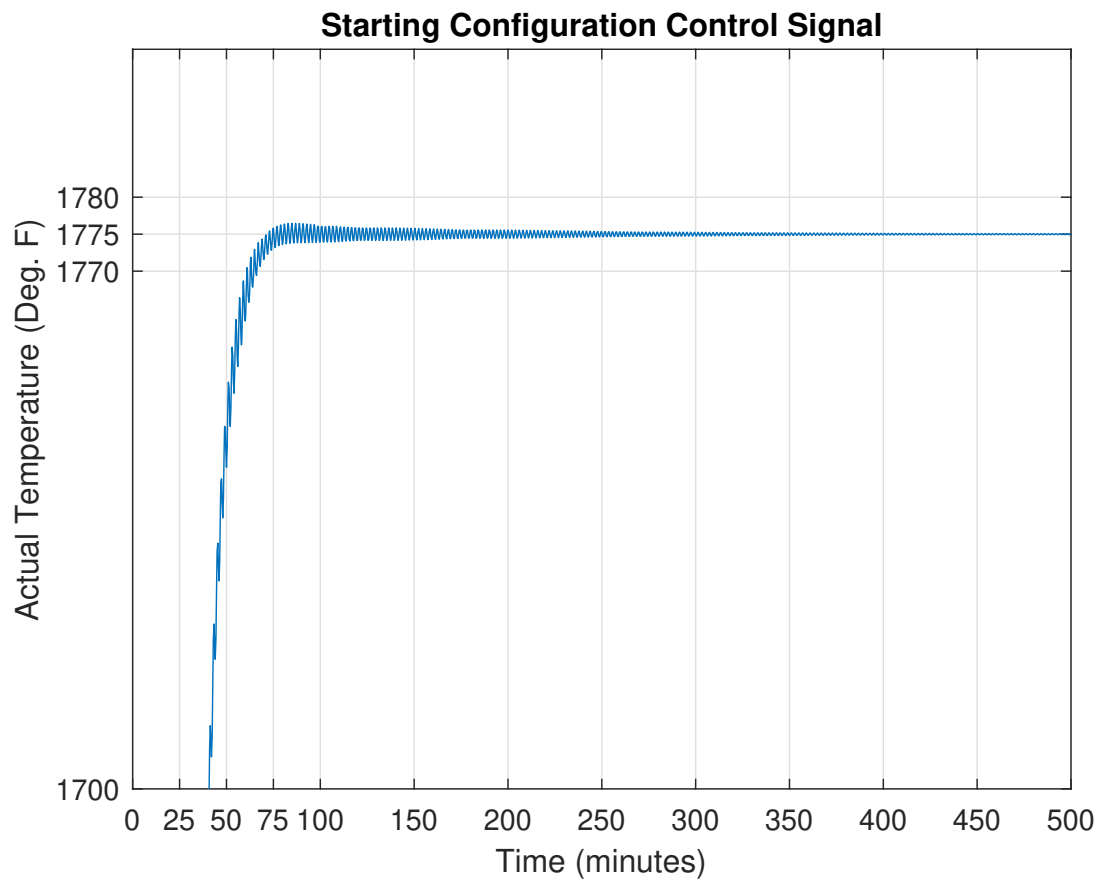


Figure 3.2: Starting PID Configuration Control Signal Response to 1775°F Step Input

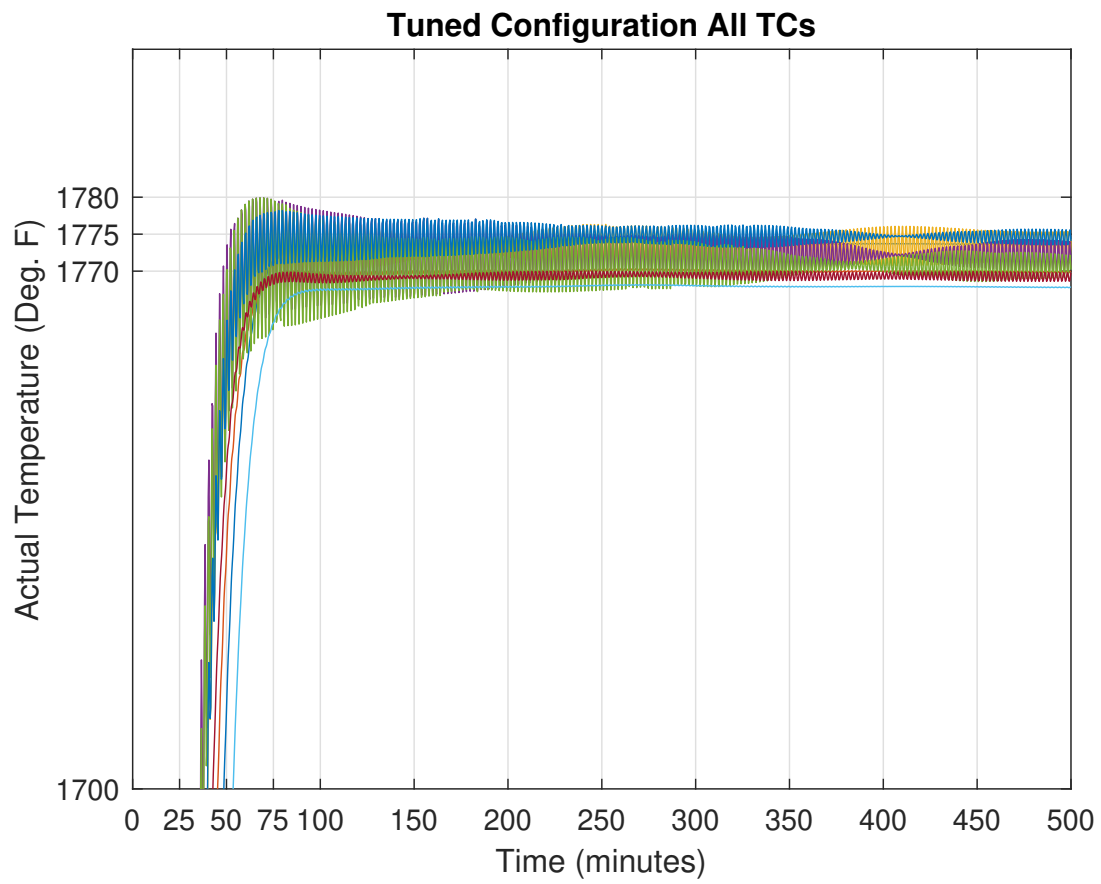


Figure 3.3: Tuned PID Configuration All TC Response to 1775°F Step Input

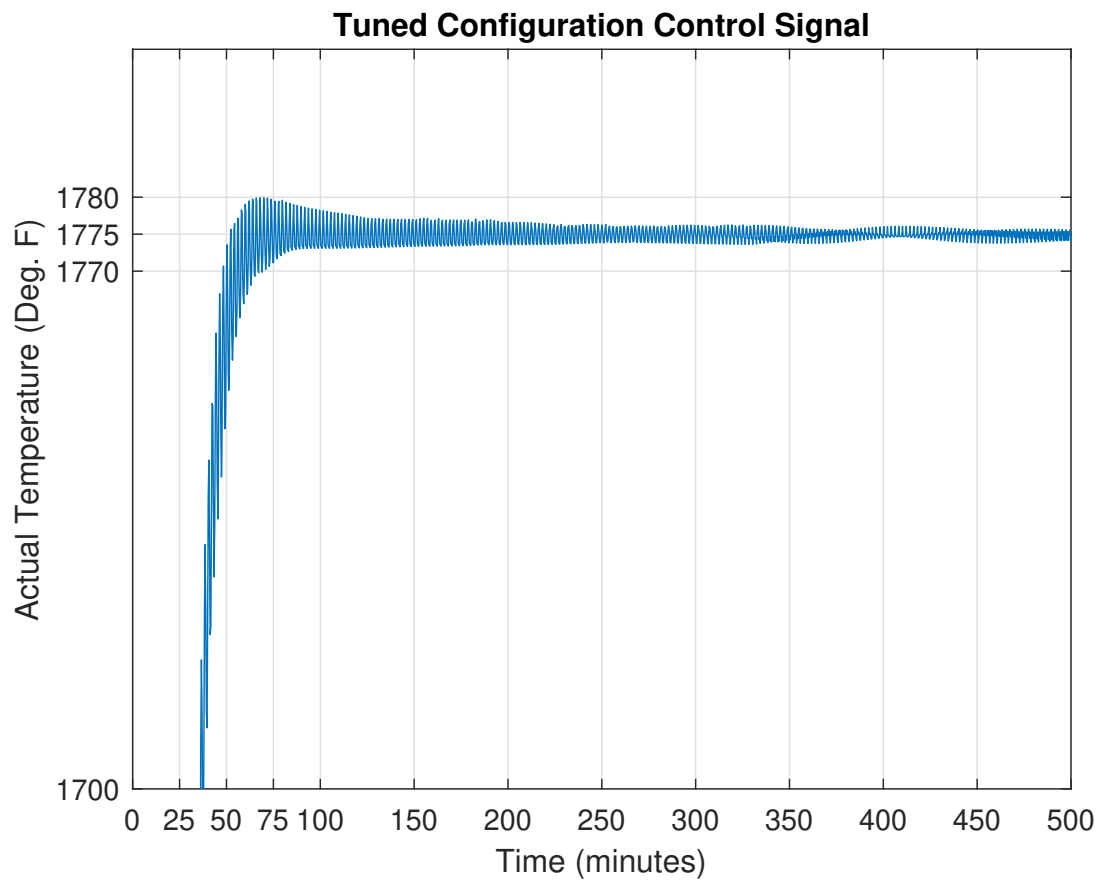


Figure 3.4: Tuned PID Configuration Control Signal Response to 1775°F Step Input

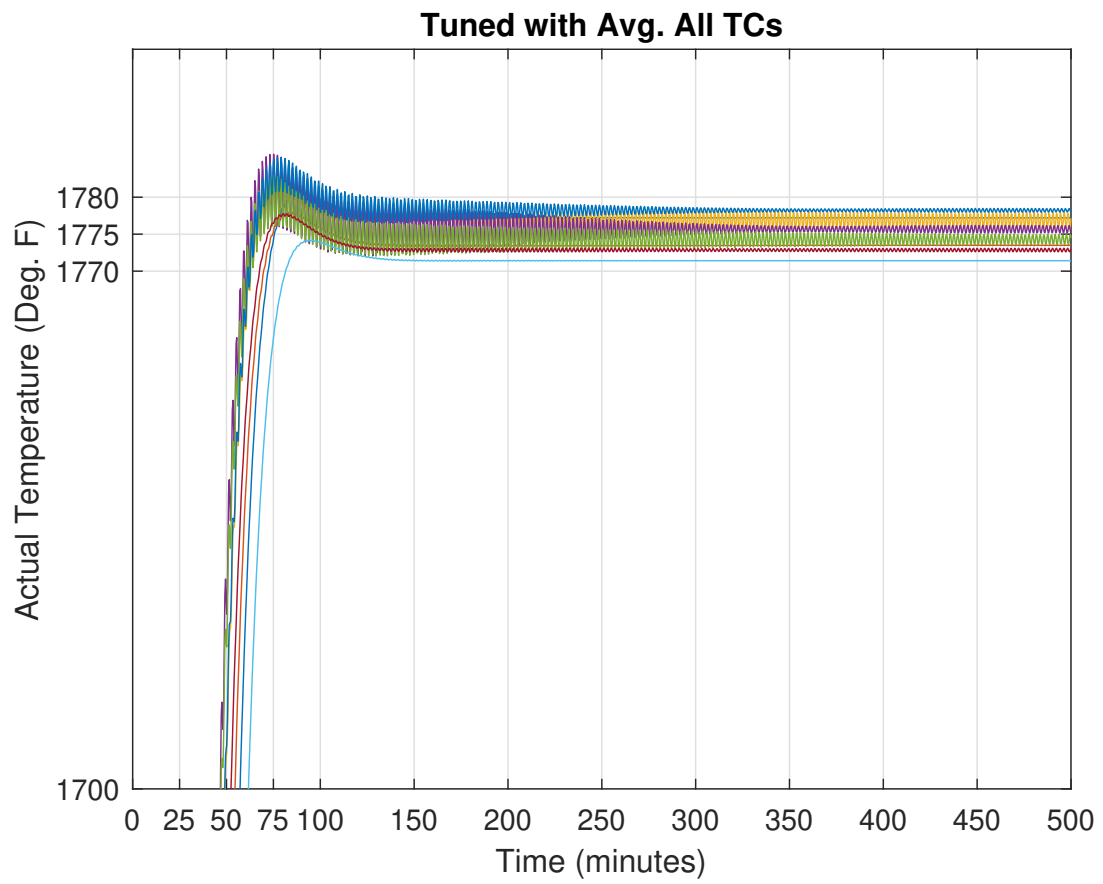


Figure 3.5: Average Temp. Signal Configuration All TC Response to $1775^{\circ}F$ Step Input

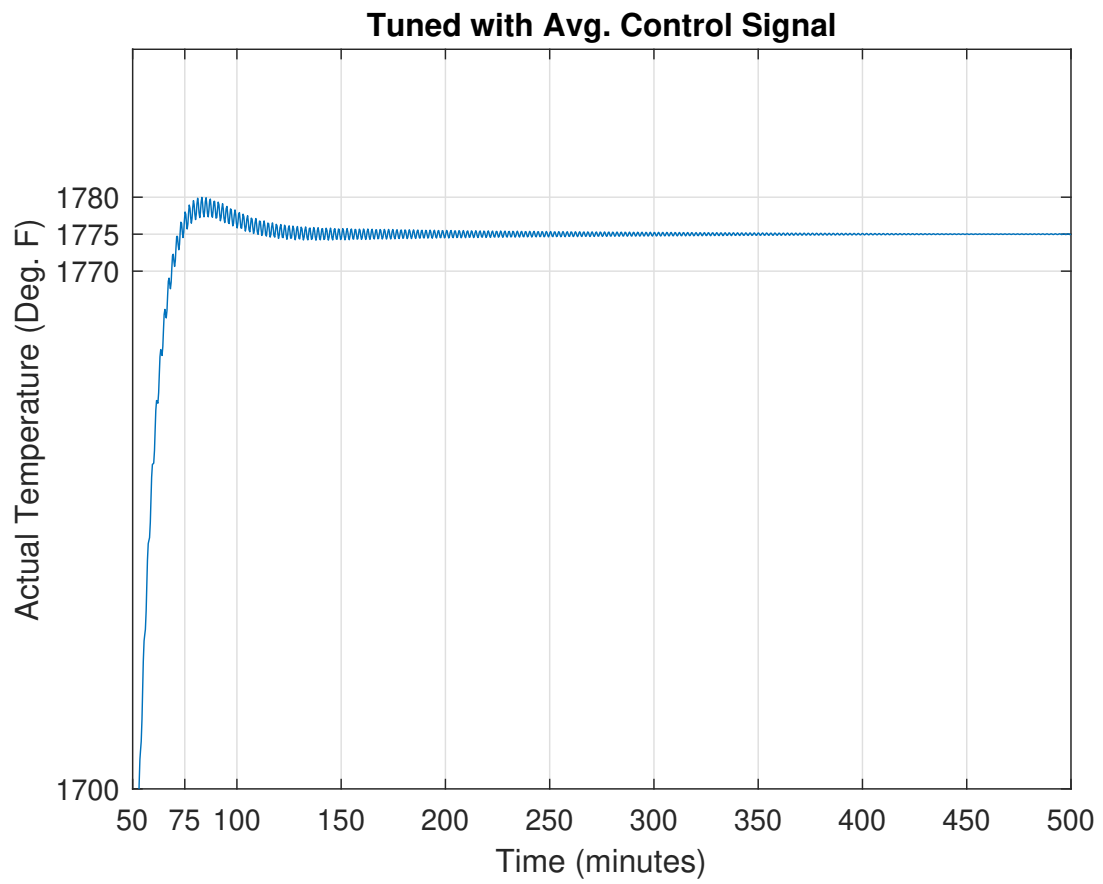


Figure 3.6: Average Temp. Configuration Control Signal Response to 1775°F Step Input

3.2 MIMO ROBUST CONTROLLER

The thermodynamic model is characterized by a 20×8 TF matrix with a high degree of coupling. Therefore the controller is a 8×20 TF matrix with measured TC zone temperatures as inputs and outputs of gas and air mass flow rates to each burner. The MATLAB function *mixsyn* was used to synthesize a H_∞ robust controller [11]. The *mixsyn* function is a mixed sensitivity loop shaping algorithm that minimizes the closed loop ($M(s)$) H_∞ norm shown in (3.3) with weighting functions W_1 , W_2 , and W_3 , sensitivity S , complementary sensitivity T , and controller K [11]. The resulting controller is 196^{th} order, and produces the closed loop response shown in Fig. 3.7 when subject to a step function from $288^\circ K$ to $1250^\circ K$. While 196^{th} order may seem excessive it is largely a result of the quantity of inputs and outputs; lower order controllers were simulated, but performance was unacceptable. The rise time of this controller is about 52 seconds and the steady-state error is about $2^\circ K$ or $4^\circ F$ which is within the TUS margin. The primary issue with this controller is that it does not account for actuator saturation. To validate the rise time is physically possible the maximum mass flow rates at 100% theoretical air were compared to the total furnace mass. At this these flow rates the burners perform a complete air changout every 90 seconds. Since the target temperature is slightly more than half the flame temperature at 100% theoretical air the rise time is within the margin of error for what is achievable.

$$M(s) = \begin{bmatrix} W_1 S \\ W_2 K S \\ W_3 T \end{bmatrix} \quad (3.3)$$

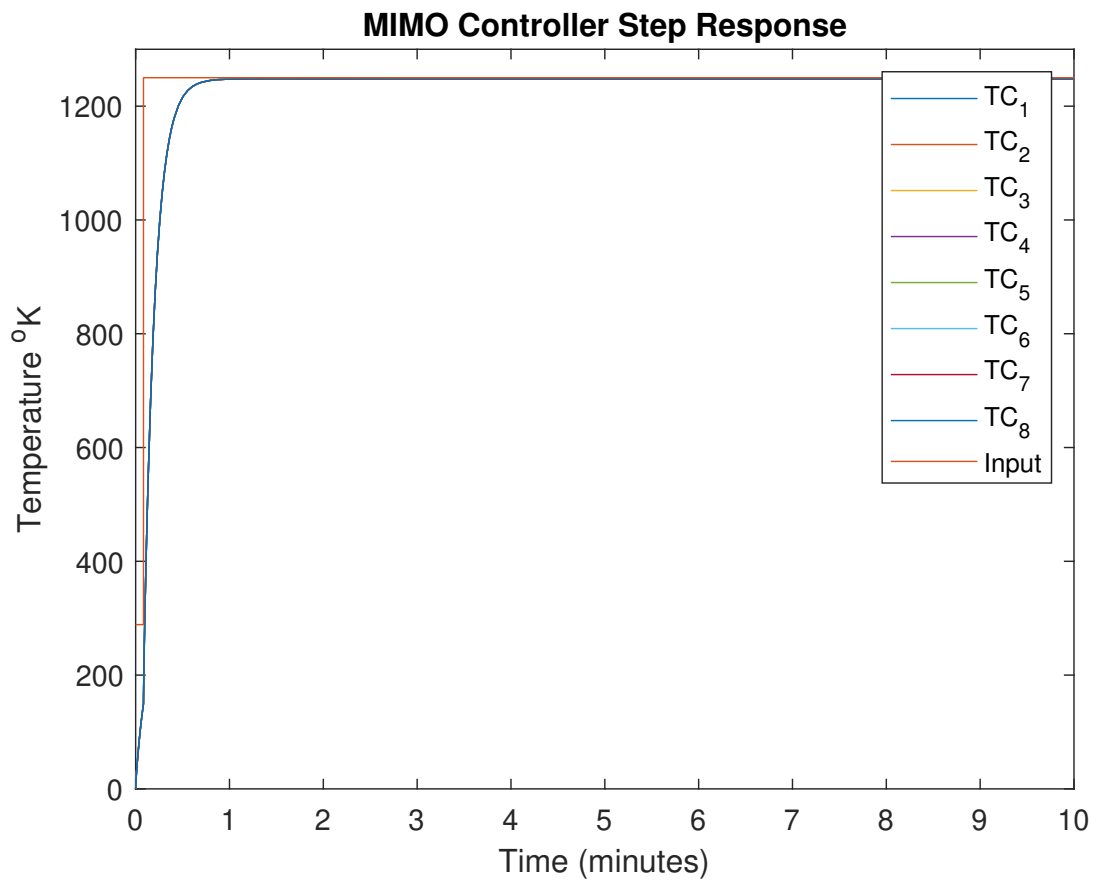


Figure 3.7: MIMO Closed Loop Step Response

CHAPTER 4: STABILITY ANALYSIS

Stability, or more relevant, margin to instability is an important factor when comparing various control schemes. A system that has good performance in a simulation environment may have small margin to instability, and thus perform poorly in an environment rife with disturbances. Two methods of stability are used to analyze the previously discussed systems.

First is the simple method of phase margin. Phase margin is calculated by $-180^\circ - \text{phase}$ at zero gain, and is easily measured via Bode plot. Typically a phase margin that balances stability and performance is 30° . Second is to apply the Nyquist Stability Criterion. Nyquist Stability Criterion states that a feedback control system is stable for the contour Γ_F , the Nyquist plot, the number of anti-clockwise encirclements of the origin of the F-plane is equal to the number of poles of F(s) in the Open Right Half Plane (ORHP)[8]. Where F(s) is the closed loop TF. This can be extended to the loop transmission function, T(s). Since $T(s) = F(s) - 1$ the Nyquist Stability Criterion dictates the anti-clockwise encirclements of the T-plane critical point, $-1 + j0$, is equal to the ORHP poles. Gershgorin analysis is a method of determining MIMO stability that plots Gershgorin circles at each point on the diagonal elements of a $n \times n$ Nyquist array. The radius of the Gershgorin circles are the sum of the magnitudes of each other element in either the same row or same column of the Nyquist array at that point. If the circles do not encircle the critical point then the MIMO system is stable. If at least one circle does encircle the critical point no definitive statement can be made regarding stability of the MIMO system[8]. The system defined with the PID controller is insufficient to make meaningful Gershgorin plots, but the MIMO controller is analyzed using Gershgorin's theorem.

4.1 PID CONTROLLER

The phase margin of these systems is calculated by producing Bode plots of each loop TF[8]. The bode plots are shown in Fig. 4.1, Fig. 4.2, and Fig. 4.3, and the phase margins are given by (4.3). Clearly all configurations have adequate phase margin.

Fig. 4.4 shows the Nyquist plot for TC_1 in the starting configuration. TC_1 is typical for the relative degree three TFs (TC_1 , TC_2 , TC_6 , and TC_7). TC_3 , TC_4 , TC_5 , and TC_8 make up a group of relative degree two TFs; the Nyquist plots for these are similar to TC_1 , but rotated 180° about the origin. The relative degree three TFs have one clockwise encirclement of the critical point, and the relative degree two TFs have no encirclements of the critical point. Therefore all the TFs are stable per the Nyquist Stability Criterion.

$$\phi_{start} = 37.5^\circ \quad (4.1)$$

$$\phi_{tuned} = 35.2^\circ \quad (4.2)$$

$$\phi_{avg} = 55.8^\circ \quad (4.3)$$

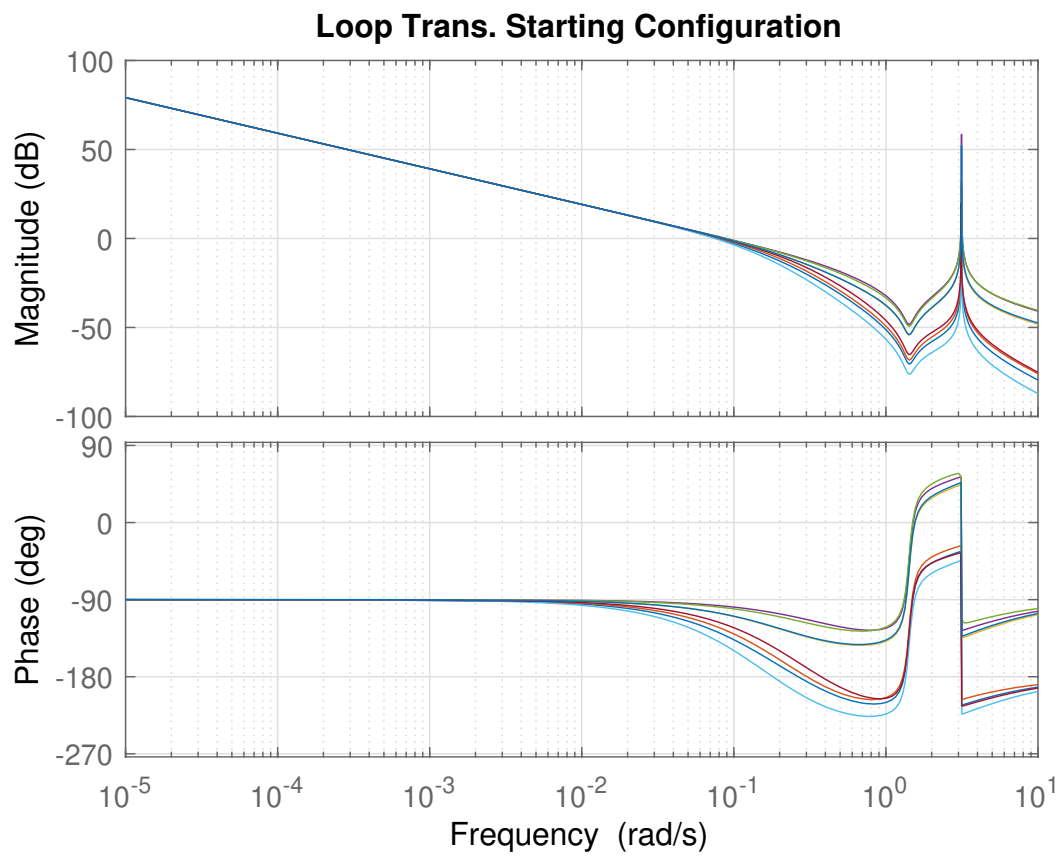


Figure 4.1: Average Temp. Configuration Control Signal Response to $1775^{\circ}F$ Step Input

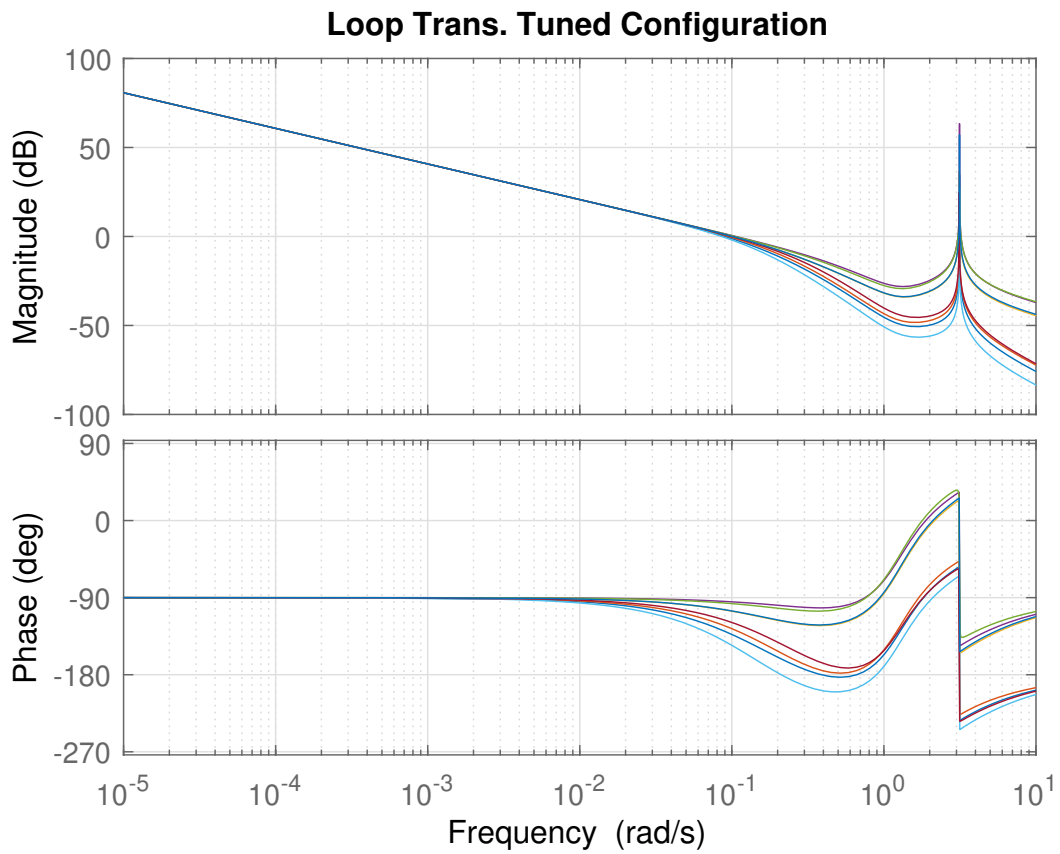


Figure 4.2: Average Temp. Configuration Control Signal Response to $1775^{\circ}F$ Step Input

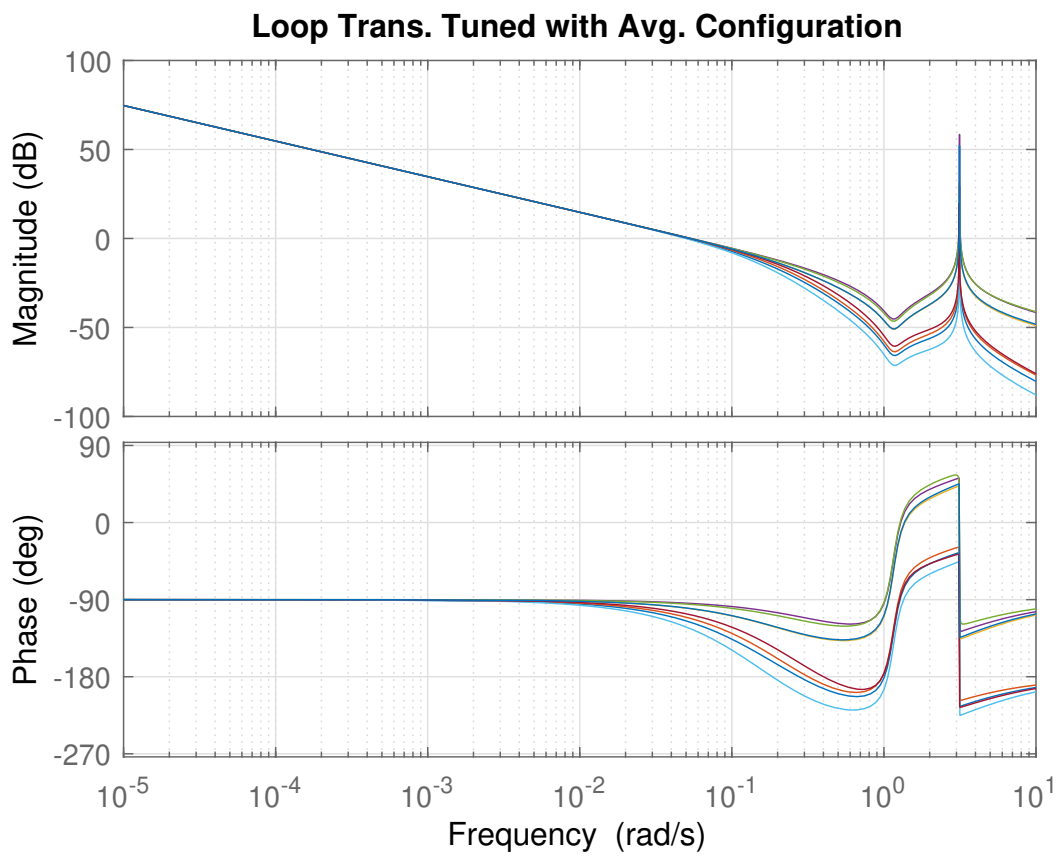
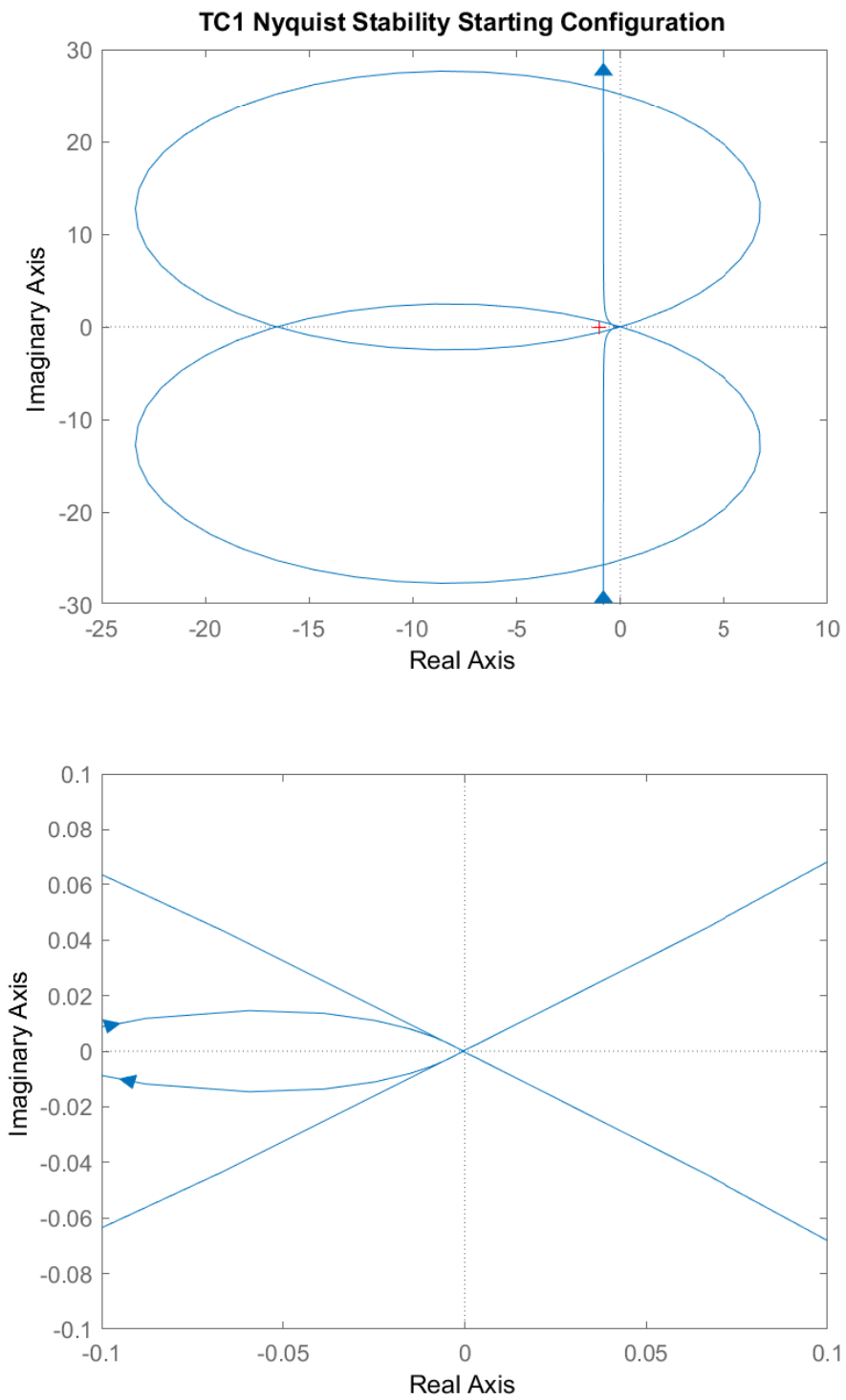


Figure 4.3: Average Temp. Configuration Control Signal Response to $1775^{\circ}F$ Step Input

Figure 4.4: TC_1 Starting Configuration Nyquist Plots

4.2 MIMO ROBUST CONTROLLER

The bode plot for the third row of the MIMO TF matrix is shown in Fig. 4.5. These are the bode plots of TC_3 output to all eight inputs. The minimum phase margin is $\phi = 91.7^\circ$ clearly all are acceptable. The other rows of loop transmission function are similar to Fig. 4.5 with the exception that some gain stabilize the entirety of some inputs; that is the magnitude of these TFs never exceed 0dB.

The Nyquist plot with Gershgorin circles is shown in Fig. 4.6. This is for location (3,3) of the loop transmission function matrix. The top graph contains the full Nyquist plot while the bottom in shows the area around the critical point. The nearly vertical lines in the top are large radius Gershgorin circles; the maximum radius is about 10^{12} . Clearly the radii become smaller near the critical point, but many Gershgorin circles do encircle the critical point. Per Gershgorin's theorem the result provides no stability information[8].

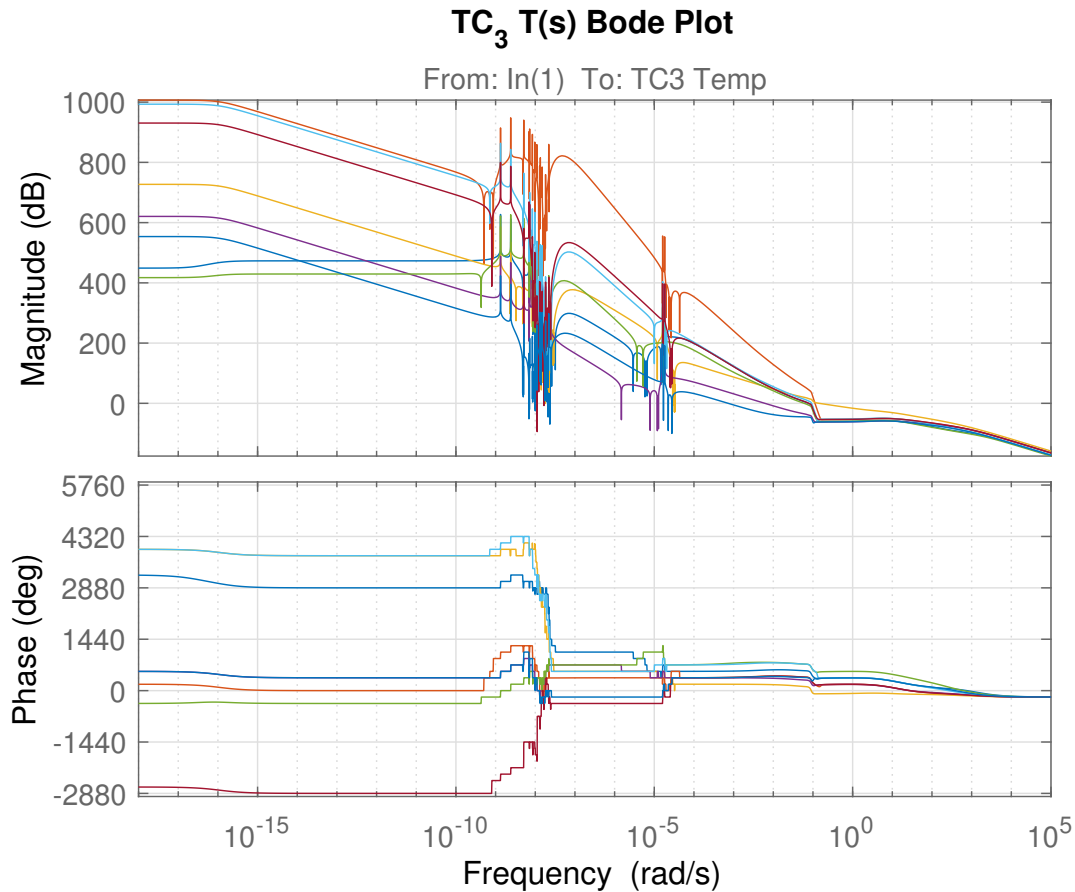


Figure 4.5: TC_3 Loop Transmission Function Bode Plots

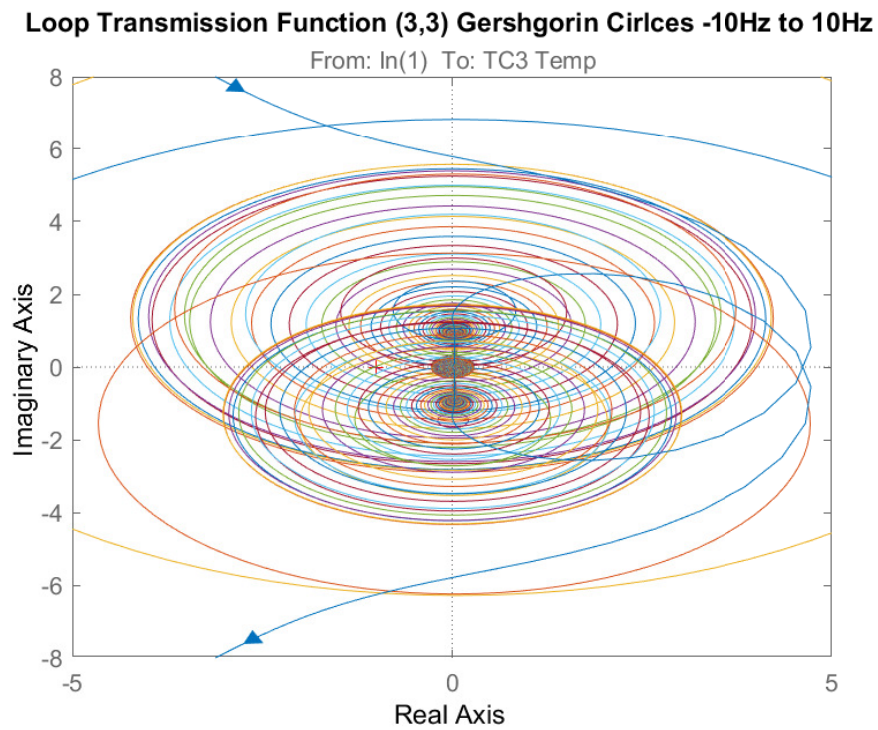
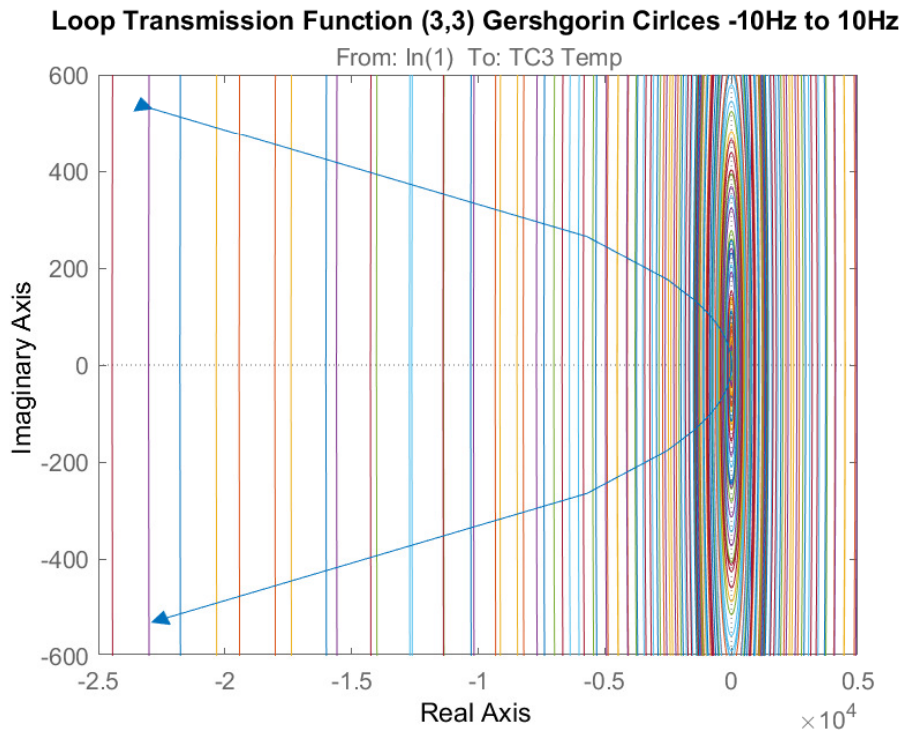


Figure 4.6: Loop Transmission Function (3,3) Gershgorin Plot

CHAPTER 5: SUMMARY AND CONCLUSIONS

The goal of this thesis is to establish a process that is usable and simply implementable by industry to improve the performance of gas fired batch heat treatment furnaces in regards to complying with Temperature Uniformity Survey (TUS) requirements and increasing product throughput. TUS are the primary method of measuring and qualifying the quality of a heat treatment furnace; in this study the closed loop systems are designed to comply with the most stringent TUS class allowing only a $\pm 5^\circ F$ steady-state error[1]. Two methods are explored to this end. The first provides a method of improving the existing system with no additional hardware changes. The second allows for hardware changes and intends to both show the relationships between physical parameters and approach the best possible product throughput. Data from a production furnace is used in the development and validation of both methods. The first method models a furnace loaded with parts while the second assumes an empty furnace.

The first method consists of using production data to generate a set of closed loop Transfer Functions (TFs), one for each Thermocouple (TC), using an output error method of system identification[7]. Knowledge of the existing Proportional, Integral, Derivative (PID) controller allows for the closed loop TFs to be converted to their open loop form. The furnace providing the data also feeds back only the maximum sensor output; this is accounted for in controller development, but is inherent in the open and closed loop TFs. With the open loop TFs known a new PID is implemented in two different scenarios. The first uses the same maximum sensor feedback and the second replaces the maximum with an average. In the first scenario the closed loop system abides by the TUS requirements and reduces the rise time by about 20%. The second closed loop system also abides by the TUS requirements but increases the rise time. The second system does reduce the steady-state temperature gradient in the furnace. Both systems are stable per the phase margin method and Nyquist stability criteria[8].

The second method treats the furnace as a Multi-Input Multi-Output (MIMO) system with each TC measurement as the outputs and combustion reactant mass flow rates as the inputs. This method splits the actuators (burners) from the plant (furnace interior), creates a time domain model of each using thermodynamic principles, simulates the time domain model to generate a frequency domain model using an output error method of system identification, and synthesizes a H_∞ robust controller using the MATLAB *mixsyn* function[7][11]. Both the time and frequency domain models are validated using TUS data. The burners are modeled by the combustion process of methane with air and the physical limitations of the burner[9][10]. For a single burner this model is a 2-input, 2-output system with the mass of methane and air as the inputs and the adiabatic flame temperature and total mass of products as the outputs. The entire bank of burners is then modeled by a 20-input, 20-output system with each burner completely decoupled from the others. The plant is built in such a way that the TC temperature exponentially rises the the adiabatic flame temperature and the time constant of the exponential is the ratio of combustion reactant mass added to the TC zone to the static mass of the zone. Coupling between burners and TC zones is determined by inspection and accounted for weighting constants. Adjacent TC zones are assumed to be coupled (i.e. they exchange air); this coupling is also modeled by weighting constants. The plant model results in a 20-input, 8-output system where the inputs to the plant are the outputs from the burners and the outputs of the plant are the TC zone temperatures. To generate

frequency domain models for the burners and plant each burner is excited separately. The burner inputs and outputs are used to generate a frequency domain model of the burner separately from the plant model. The burner outputs and plant outputs are then used to generate a frequency domain model of the plant. In TF form the burner bank is a 20×20 TF matrix with 2×2 diagonal elements representing each burner and zeros otherwise. The plant is a 8×20 TF matrix with each row representing a TC and each column a different burner output such that first two columns are the adiabatic flame temperature and reactant mass from burner one. The MATLAB *mixsyn* function is used to create a controller[11]. This controller results in a rise time of about 50 seconds and a steady state error of approximately $4^\circ F$, but does not account for actuator saturation. The controller is stable per phase margin but inconclusive per Gershgorin's theorem[8].

As shown in this thesis it is possible to improve industrial gas fired batch heat treatment furnace performance while maintaining compliance with TUS requirements. The methods discussed can be improved upon by generating data that is better suited to system identification techniques and specifically open loop data. Challenging and incorporating assumptions into the model will also improve fidelity.

REFERENCES

- [1] "Aerospace Material Specification (R) Pyrometry," SAE AMS2750 Rev. E, July 2012.
- [2] H. S. Ko, J. Kim, T. Yoon, M. Lim, D. R. Yang, I. S Jun, "Modeling and Predictive Control of a Reheating Furnace," Proceedings of the American Control Conference, Chicago, IL., June 2000.
- [3] X. Li, Haiyan Sun, Naijie Xia and Haibo Wang, "Predictive decoupling control for vacuum heat treatment furnace," 2011 IEEE International Conference on Computer Science and Automation Engineering, Shanghai, 2011, pp. 337-342.
- [4] X. Bai et al., "Measurement of coal particle combustion behaviors in a drop tube furnace through high-speed imaging and image processing," 2016 IEEE International Instrumentation and Measurement Technology Conference Proceedings, Taipei, 2016, pp. 1-6.
- [5] S. Strommer, A. Steinboeck, C. Begle, M. Niederer and A. Kugi, "Modeling and control of gas supply for burners in gas-fired industrial furnaces," 2014 IEEE Conference on Control Applications (CCA), Juan Les Antibes, 2014, pp. 210-215.
- [6] V. Demidovich, Y. Perevalov and G. Prokofiev, "Temperature Control Systems in Continuous Heat Treatment Lines," 2019 XXI International Conference Complex Systems: Control and Modeling Problems (CSCMP), Samara, Russia, 2019, pp. 424-428.
- [7] A. K. Tangirala, "Principles of System Identification Theory and Practice," CRC Press, Boca Raton, FL, 2015.
- [8] J. O'Brien, "Frequency Domain Control for High-Performance Systems," Institute for Engineering and Technology, London, United Kingdom, 2012.
- [9] C. Borgnakke, R. E. Sonntag, "Fundamentals of Thermodynamics Seventh Ed. Chapter 15: Chemical Reactions", John Wiley Sons, Inc. 2009.
- [10] Hauck Manufacturing Co. "SVG Super Versatile Gas Burner, Burner Model 115B" Supplemental Data, Aug. 2009.
- [11] www.mathworks.com
- [12] Unifrax LLC. "Fiberfrax Blanket and Mat Products, Product Information Sheet, Durablanket 2600", June 2017.